International Journal for Parasitology 50 (2020) 235–252

Contents lists available at ScienceDirect

International Journal for Parasitology

journal homepage: www.elsevier.com/locate/ijpara

# Screening the Medicines for Malaria Venture Pathogen Box for invasion and egress inhibitors of the blood stage of *Plasmodium falciparum* reveals several inhibitory compounds

Madeline G. Dans [a,b,*], Greta E. Weiss [a], Danny W. Wilson [c,a], Brad E. Sleebs [d,e], Brendan S. Crabb [a,e], Tania F. de Koning-Ward [b], Paul R. Gilson [a,*]

[a] Burnet Institute, Melbourne, Victoria 3004, Australia
[b] School of Medicine, Deakin University, Waurn Ponds, Victoria 3216, Australia
[c] Research Centre for Infectious Diseases, The University of Adelaide, Adelaide, South Australia 5005, Australia
[d] Walter and Eliza Hall Institute, Parkville, Victoria 3052, Australia
[e] The University of Melbourne, Parkville, Victoria 3010, Australia

ARTICLE INFO

*Article history:*
Received 15 September 2019
Received in revised form 30 December 2019
Accepted 5 January 2020
Available online 3 March 2020

*Keywords:*
*Plasmodium falciparum*
Pathogen Box
Invasion
Egress
Drug screen

ABSTRACT

With emerging resistance to frontline treatments, it is vital that new drugs are identified to target *Plasmodium falciparum*. One of the most critical processes during parasites asexual lifecycle is the invasion and subsequent egress of red blood cells (RBCs). Many unique parasite ligands, receptors and enzymes are employed during egress and invasion that are essential for parasite proliferation and survival, therefore making these processes druggable targets. To identify potential inhibitors of egress and invasion, we screened the Medicines for Malaria Venture Pathogen Box, a 400 compound library against neglected tropical diseases, including 125 with antimalarial activity. For this screen, we utilised transgenic parasites expressing a bioluminescent reporter, nanoluciferase (Nluc), to measure inhibition of parasite egress and invasion in the presence of the Pathogen Box compounds. At a concentration of 2 μM, we found 15 compounds that inhibited parasite egress by >40% and 24 invasion-specific compounds that inhibited invasion by >90%. We further characterised 11 of these inhibitors through cell-based assays and live cell microscopy, and found two compounds that inhibited merozoite maturation in schizonts, one compound that inhibited merozoite egress, one compound that directly inhibited parasite invasion and one compound that slowed down invasion and arrested ring formation. The remaining compounds were general growth inhibitors that acted during the egress and invasion phase of the cell cycle. We found the sulfonylpiperazine, MMV020291, to be the most invasion-specific inhibitor, blocking successful merozoite internalisation within human RBCs and having no substantial effect on other stages of the cell cycle. This has significant implications for the possible development of an invasion-specific inhibitor as an antimalarial in a combination based therapy, in addition to being a useful tool for studying the biology of the invading parasite.


## 1. Introduction

Malaria remains a significant global health burden with an estimated 228 million cases worldwide in 2018, resulting in 405,000 deaths (World Health Organization, 2019). Of the *Plasmodium* spp. known to infect humans, *Plasmodium falciparum* remains the deadliest and is therefore a focus in the fight to eradicate malaria. There is emerging resistance of *P. falciparum* to the gold standard artemisinin combination therapies (ACTs) whereby delayed parasite clearance has been observed in regions of southeastern Asia (Dondorp et al., 2009; Fairhurst and Dondorp, 2016; Vijaykadga et al., 2006; World Health Organization, 2019). With the spread of resistance to artemisinin and its partner drugs, it is vital that novel therapeutics are developed and ready to deploy when ACTs are rendered ineffective.

The red blood cell (RBC) stage of infection causes the clinical symptoms of malaria. Asexual blood stage parasites progress through a series of developmental phases that begin with the intracellular ring stage, followed by the trophozoite stage and concludes

* Corresponding authors at: Burnet Institute, Melbourne, Victoria 3004, Australia (M.G. Dans).
*E-mail addresses:* madeline.dans@burnet.edu.au (M.G. Dans), paul.gilson@burnet.edu.au (P.R. Gilson).

https://doi.org/10.1016/j.ijpara.2020.01.002
0020-7519/

with the DNA-replicative schizont phase. From mature schizonts, approximately 20 invasive merozoites egress from the nutrient-deprived infected RBC (iRBC) after the breakdown of the parasitophorous vacuole membrane (PVM), followed by the rupture of the RBC membrane (Wickham et al., 2003; Chandramohanadas et al., 2011). Egress appears to be initiated via the activation of cGMP dependent protein kinase G (PKG), which has been shown to be specifically inhibited by the trisubstituted pyrrole, Compound 1 (C1) (Gurnett et al., 2002; Taylor et al., 2010; Hopp et al., 2012). Activated PKG triggers the discharge of the serine subtilisin-like protease (SUB1) from the exonemes (Yeoh et al., 2007; Collins et al., 2013) that undergoes autoprocessing in the endoplasmic reticulum (ER) (Blackman et al., 1998; Sajid et al., 2000), followed by a second processing event, requiring the aspartic protease, plasmepsin X (PMX) (Nasamu et al., 2017; Pino et al., 2017). Secretion of mature SUB1 into the parasitophorous vacuole (PV) induces the processing of serine rich antigen 5 and 6 proteins (SERA5/6) (Yeoh et al., 2007; Ruecker et al., 2012; Collins et al., 2013; Collins et al., 2017; Thomas et al., 2018), merozoite surface protein 1 (MSP1) (Das et al., 2015), as well as other merozoite surface proteins (Koussis et al., 2009; Silmon de Monerri et al., 2011). Permeabilisation of the PVM occurs 10–30 min prior to PKG activation of SUB1, indicating that there are other unknown effector molecules required for PVM fragmentation (Hale et al., 2017). Both SUB1-activated SERA6 and MSP1 have both been implicated in disrupting the RBC membrane to allow egress of merozoites via cleavage and binding of spectrin within RBCs, respectively (Das et al., 2015; Thomas et al., 2018). Furthermore, a conditional knockdown of SERA6 elucidated a similar phenotype to the cysteine protease inhibitor, E64, whereby PVM rupture occurred but the RBC membrane remained intact (Glushakova et al., 2009; Thomas et al., 2018). Other regulatory enzymes such as calcium dependent kinases 1 and 5 (CDPK1/5) have also been implicated as important mediators of signalling cascades to allow merozoite egress (Dvorin et al., 2010; Iyer et al., 2018). Recently, it has been shown that CDPK5 is required for the discharge of micronemes and may be involved in a partnership with PKG to 'enhance' the cascade of events that eventuate in the release of invasive merozoites (Absalon et al., 2018). Following egress, the merozoite secretes proteins from its unique secretory organelles; the rhoptries and micronemes, which enable the merozoite to invade new RBCs in a complex multi-step process that is still not fully understood (Sam-Yellowe, 1996; Bannister et al., 2000; Farrow et al., 2011). The primary contact between a merozoite and a RBC occurs via a multi-protein complex containing MSP1 (Holder and Freeman, 1984; Lin et al., 2014) and possibly heparin sulfate proteoglycan receptors on the RBC surface, since heparin inhibits this interaction (Vogt et al., 2004; Boyle et al., 2017). Subsequent stronger attachment between merozoites and RBCs is through the binding of merozoite proteins, namely, reticulocyte binding like homologs (Rhs) and erythrocyte binding proteins (EBAs), which are secreted from the rhoptries and micronemes, respectively (Camus and Hadley, 1985; Mayer et al., 2001; Lanzillotti and Coetzer, 2006; Li et al., 2012). Downstream binding of Rh5 to the RBC receptor, basigin, then possibly activates the secretion of the rhoptry neck protein complex (RON) which becomes embedded into the RBC surface (Weiss et al., 2015). Here, RON2 interacts with apical membrane antigen 1 (AMA1) which is secreted from the micronemes onto the merozoite surface, leading to the formation of a tight junction between the invading merozoite and RBC (Cao et al., 2009; Lamarque et al., 2011). The parasite's actin-myosin motor applies a penetrative force to propel the merozoite into the RBC, during which the merozoite envelops itself in the RBC membrane, forming the PVM (Dobrowolski and Sibley, 1996; Gonzalez et al., 2009). Less than 1 min after invasion, the RBC undergoes echinocytosis, a morphological change from its normal biconcave shape to a stellate form, hypothesised to be caused by an efflux of ions or a disruption to the phospholipid bilayer of the RBC upon secretion of rhoptry proteins (Gilson and Crabb, 2009; Weiss et al., 2015; Weiss et al., 2016). Since many of the protein–protein interactions, signalling cascades and enzymes required for egress and invasion are unique to parasites, they could represent novel drug targets that may be effective antimalarials when used in combination with drugs that act during the intraerythrocytic stage (reviewed in (Burns et al., 2019)).

To facilitate open source drug discovery for antimalarials, Medicines for Malaria Venture (MMV) has released a series of small compound libraries, screened for their ability to inhibit the RBC stage of the parasite's lifecycle (http://www.mmv.org/research-development). The first compound library, termed the Malaria Box (Van Voorhis et al., 2016), was phenotypically screened by Subramanian et al. (2018) for blood stage egress and invasion inhibitors which resulted in the identification of 26 compounds that inhibited schizont to ring transition by greater than 50% (Subramanian et al., 2018). The second generation library released by MMV was labelled the Pathogen Box, and it contains 400 compounds against neglected tropical diseases, 125 from the Malaria disease set and 15 with activity against the related parasite, *Toxoplasma gondii*. To date, the Pathogen Box has been a useful tool in high throughput screens (HTS), with many compounds identified as inhibitors of a variety of disease causing organisms (Duffy et al., 2017; Hennessey et al., 2018; Spalenka et al., 2018; Tong et al., 2018; Nugraha et al., 2019; Nyagwange et al., 2019; Wang et al., 2019). We have screened the Pathogen Box using a bioluminescent semi-high throughput system to identify inhibitors of RBC egress and invasion, identifying 15 and 24 inhibitors, respectively, with these properties. After removing compounds with known, non-invasion related targets or those that did not inhibit parasite growth, we performed a detailed analysis of 11 of these compounds by studying their effects upon egress and invasion.

## 2. Materials and methods

### 2.1. Parasite culture and strains

*Plasmodium falciparum* parasites were continuously cultured as previously described (Trager and Jensen, 1976) in human RBCs (Australian Red Cross Blood Bank, Type O) at 4% haematocrit in supplemented RPMI medium (RPMI (Sigma, UK), HEPES (GIBCO, USA), 0.2% $NaHCO_3$ (Thermo Scientific, Australia), 5% heat-inactivated human serum (Australian Red Cross), 0.25% AlbumaxII (GIBCO, New Zealand), 0.37 mM hypoxanthine (Sigma, USA), 31.25 μg/mL of Gentamicin (GIBCO, USA)) at 37 °C. An exported Nluc parasite line (PEXEL-Nluc) was used as previously described (Azevedo et al., 2014), which was generated by transfecting a Hyp1-Nluc plasmid under the control of an *ef1α* promoter into 3D7 *P. falciparum* parasites (Hasenkamp et al., 2012). Uptake of the plasmid was selected for and maintained by 2.5 nM WR99210 (Jacobus, USA). This parasite line was used for all experiments in the study.

### 2.2. Compounds

Pathogen Box compounds were obtained from MMV and consisted of 400 compounds at 10 mM dissolved in DMSO (https://www.pathogenbox.org/). Compounds were diluted to 100 μM and aliquoted into 96 well plates at −80 °C for long-term storage. The compounds were then diluted to a final concentration of 2 μM in RPMI medium for the screen and early ring inhibition assay, with a final concentration of 0.02% DMSO. Further quantities of

MMV011765, MMV637229, MMV020291, MMV006833, MMV688279, MMV676877 and MMV676881 were provided by MMV and MMV016838 (MolPort-001-614-591), MMV020512 (MolPort-004-158-754), MMV019721 (MolPort-004-102-322) and MMV687794 (MolPort-002-553-011) were purchased from Molport. R1 peptide (a kind gift from Alan Cowman, Walter and Eliza Hall Institute, Australia) and porcine heparin (Sigma, USA) were dissolved in RPMI medium. Chloroquine (Sigma, USA) and E64 (Sigma, USA) were dissolved in water. Artemisinin (Sigma, USA) and Compound 1 (custom made) and all other compounds were dissolved in DMSO. In all experiments, heparin was used at 100 μg/mL (Boyle et al., 2010a), Compound 1 at 4 μM (10 × $EC_{50}$ of egress as determined in Supplementary Fig. S1A) and E64 at 10 μM (Glushakova et al., 2009). In order to minimise non-specific invasion or egress inhibition due to potency, antimalarials chloroquine and artemisinin were used at 5 × $EC_{50}$ of growth which corresponded to 75 nM and 15 nM, respectively.

### 2.3. Nanoluciferase invasion assay and statistical validation for a high throughput screen

Parasites were grown to late stage schizonts and isolated using a Percoll density gradient whereby culture was added to 60% buffered Percoll solution in supplemented RPMI (10 mM $NaH_2PO_4$, 143 mM NaCl, Percoll (GE Healthcare Bio-Sciences, Sweden)). Purified schizonts at 1–2% parasitemia were added to RBCs with a final haematocrit of 1%. Drugs were administered at concentrations of 0.02%, 4 μM and 100 μg/mL for DMSO, C1 and heparin, respectively. Plates were incubated at 37 °C for 4 h and the growth medium was removed to measure Nluc released upon merozoite egress (see section 2.4). This time frame was chosen as it allowed sufficient egress and invasion events to occur and produce a robust invasion signal, whilst minimising the exposure time of newly invaded ring-stage parasites to the inhibitors that could produce false positives for invasion inhibition. Cells were treated with sorbitol to induce osmotic lysis of remaining schizonts, and three washes were performed before incubating the culture at 37 °C for a further 24 h until parasites were >24 h post invasion. Whole cells were lysed to measure intracellular Nluc, corresponding with initial invasion rate (see Section 2.4). A background control was included for the egress measurements which consisted of the growth media of Percoll purified cultures that had been kept at 4 °C during the first 4 h incubation period. This allowed a baseline level of Nluc to be established to ensure the signal measured was attributed to schizont rupture and not spontaneous lysis or cell leakage. To account for contamination of ring stage parasites that failed to be removed from Percoll gradient and schizonts that failed to be removed by sorbitol treatment, a background control for the invasion measurements was included whereby Percoll purified cultures were kept at 4 °C during the first 4 h incubation and subsequently treated with sorbitol before further incubation at 37 °C for 24 h.

### 2.4. Measuring nanoluciferase activity

Whole cells (5 μL) at 1% hematocrit (invasion) or growth medium (egress) were dispensed into white 96 well luminometer plates and 45 μL of 1 × NanoGlo Lysis Buffer containing 1:1000 NanoGlo substrate (Promega, USA) was injected into wells. Relative light units (RLU) was measured by a CLARIOstar luminometer (BMG Labtech).

#### 2.4.1. Analysis

The percent of invasion/egress was determined as described in the formula below:

$$Invasion\ or\ Egress(\%) = \frac{(RLU_{AV\ Treated} - RLU_{AV\ background\ control\ (egress\ or\ invasion)})}{(RLU_{AV\ UT} - RLU_{AV\ background\ control\ (egress\ or\ invasion)})} X100$$

The mean and S.D. of 60 total wells (15 wells per plate over four biological replicates) for each drug treatment was used to calculate Z factors. DMSO, heparin and C1 treatments were first normalised to the untreated control and values were input into the following equation as per (Zhang et al., 1999):

$$Z = 1 - \frac{3S.D._{Heparin/C1} + 3S.D._{DMSO}}{abs(mean_{Heparin/C1} - mean_{DMSO})}$$

### 2.5. Screening the Pathogen Box

The Nanoluciferase invasion assay was used as described above. Pathogen Box compounds were diluted to a final concentration of 2 μM with concentrations of DMSO, C1 and heparin as listed above. Chloroquine was included at 75 nM. Each plate contained 40 compounds in duplicate with control compounds. The percentage of invasion and egress in the presence of compounds was normalised relative to the mean of DMSO (100% egress or invasion rate) that was averaged across three biological replicates.

### 2.6. Counter screen

Parasites were grown to 24 h post invasion and adjusted to a final haematocrit of 1% with 1–2% parasitemia. Cells were lysed in 1× Nanoglo Lysis Buffer (Promega) and lysate was added to 10 μM of the Pathogen Box compounds and incubated for 10 min at 37 °C. Nanoluciferase activity was measured as above with 45 μL of lysate dispensed into 96 well white luminometer plates and 5 μL of 1:100 NanoGlo substrate injected into wells. Nluc activity in presence of compounds was normalised relative to 0.1% DMSO (100% Nluc activity).

### 2.7. Early ring inhibition assay

This was performed as per the Nluc invasion assay with Pathogen Box compounds tested at a concentration of 2 μM. Chloroquine and artemisinin were included at concentrations of 75 nM and 25 nM, respectively. Duplicate wells for each compound were set up, one that received drug treatment during the egress/invasion window and one that remained untreated. After the 4 h incubation, following sorbitol treatment and washes, the well that was untreated received drug treatment for a further 4 h before being washed three times. At 24 h post invasion, cultures were lysed and Nluc activity measured as described above. Percentage of invasion and early ring growth in the presence of compounds was normalised relative to 0.02% DMSO (100% invasion or early ring growth).

### 2.8. Egress inhibition reversibility assay

Schizonts were Percoll purified as described above and cultured in 1% haematocrit of 1–2% parasitemia. To this, C1, MMV011765, MMV016838 and DMSO were added at final concentrations of 4 μM, 10 μM, 10 μM and 0.1%, respectively. Plates were incubated for 2 h at 37 °C before growth medium was collected. Pellets were washed three times and incubated for a further 4 h at 37 °C before growth medium was collected. Nluc released in the growth medium was measured as described above. Egress was normalised relative to 0.1% DMSO after 2 h and normalised to cumulative 0.1% DMSO after 4 h (i.e. 2 h + 4 h DMSO RLU).

### 2.9. Merozoite invasion assay

Adapted from (Boyle et al., 2010b; Wilson et al., 2013, 2015) where parasites were grown to schizonts, magnet purified and treated with 10 μM E64 (or 10 μM MMV676881) for 4–6 h until >50% had become RBC membrane (RBCM) trapped merozoites. Schizonts were washed with supplemented RPMI before being mechanically disrupted by passage through a 1.2 μm filter and distributed into a 96-well plate with a final hematocrit of 1% and ~10 × $EC_{50}$ of growth of each drug (10 μM MMV020291, 3 μM MMV006833, 3 μM MMV668279, 7 μM MMV676877, 3 μM MMV687794, 5 μM MMV020512, 5 μM MMV019721, 10 μM MMV637229 (5 × $EC_{50}$)). The 96-well plate was shaken at 400 rpm for 30 min at 37 °C. Pellets were washed three times and put back into culture for 24 h before Nluc activity was measured as described above. Invasion was normalised relative to 0.1% DMSO.

### 2.10. Trophozoite growth assays

Hyp1-Nluc parasites at ~24 h post invasion were adjusted to 1% parasitemia and 1% haematocrit in a 96-well plate before being exposed to 10 × $EC_{50}$ of Pathogen Box compounds for 4 h. Plates were then washed three times in supplemented RPMI before being put back into culture until the following cycle. Growth was calculated at ~24 h post invasion by measuring Nluc activity as described above. C1, heparin, chloroquine and artemisinin were included as controls at 4 μM, 100 μg/mL, 75 nM and 25 nM, respectively. Values were normalised to 0.1% DMSO as a vehicle control.

### 2.11. Determination of $EC_{50}$s for parasite invasion and egress of RBCs

Compounds were serially diluted from 10 μM and rates of parasite egress and invasion were measured by the Nluc invasion assay as described above. Percentage of invasion and egress in the presence of compounds was normalised to 0.1% DMSO (100% invasion or egress rate). Curves were then normalised between 0 and 100%. $EC_{50}$ curves were generated from GraphPad Prism using a non-linear regression.

### 2.12. Live cell microscopy

Live cell microscopy was performed as described in Crick et al. (2013) and Weiss et al. (2015) on a Zeiss Cell Observer widefield fluorescent microscope equipped with a humidified gas chamber (1% $O_2$, 5% $CO_2$ and 94% $N_2$) at 37 °C. Eight well LabTek chambered slides were filled with 200 μL of parasite culture, diluted to a final 0.1% haematocrit in RPMI medium and treated with 10 × $EC_{50}$ of compound. Mature schizonts that appeared to rupture were imaged at two to four frames per s using the AxioCam 702 Mono camera for 20 min. Image and data analysis of cell behaviour was performed using ImageJ and GraphPad Prism with statistical tests between treated and vehicle control including unpaired *t* tests (for normally distributed data) and Mann-Whitney *t* test (for non-normally distributed data).

### 2.13. Bodipy staining

RBCs at 1% haematocrit were stained with bodipy sphingomyelin green (Life Technologies, Australia) diluted 1:500 in RPMI by incubating overnight at 37 °C. Trophozoites were incubated with 1:1000 bodipy ceramide Texas red (Life Technologies, Australia) overnight in RPMI as described above but without human serum and decreased Albumax (0.125%). Approximately 12 h later, schizonts were Percoll purified as described above and stained RBCs were washed twice in RPMI. Schizonts and RBCs were combined and then imaged as described above for live cell microscopy conditions.

## 3. Results

### 3.1. Development and validation of bioluminescent egress and invasion screening assay

To screen the MMV Pathogen Box for egress and invasion inhibitors, we used *P. falciparum* 3D7 parasites expressing a Nanoluciferase (Nluc) that is exported into the cytoplasmic compartment of the iRBC (previously described in Azevedo et al. (2014)) in an assay we termed the Nluc invasion assay (Fig. 1A). Briefly, in this assay late stage schizonts were purified and added to RBCs in the presence of inhibitors for 4 h. The culture medium was then collected to measure bioluminescence in RLU of the Nluc released upon schizont rupture. The iRBCs were then treated with 5% isotonic sorbitol to lyse remaining schizonts, leaving intact newly invaded ring stage parasites. Since it was not possible to measure Nluc in the new ring stage parasites as Nluc expression was too low (Azevedo et al., 2014), the iRBCs were grown for ~24 h until trophozoites (parasite age range 24–28 h post invasion). The trophozoite iRBCs were then lysed and degree of invasion was inferred by RLU levels.

To validate the suitability of this assay for HTS, we generated Z-factors using the well-characterised egress and invasion inhibitors, C1 and heparin, respectively, as positive controls for inhibition of egress and invasion, respectively (Zhang et al., 1999; Gurnett et al., 2002; Hopp et al., 2012; Weiss et al., 2015; Boyle et al., 2017). For both egress and invasion, the assay achieved moderate separation bands between its positive (C1 and heparin) and negative drug vehicle DMSO control, producing Z-factors for egress and invasion of 0.39 and 0.49, respectively (Fig. 1B). Whilst the ideal Z-factor for an assay to be used in a HTS is >0.5, the Z-factors we achieved in the Nluc invasion assay were on the threshold to distinguish positive from negative hit compounds. However, due to the small size of the Pathogen Box, we felt that it was an acceptable method to use as we could conduct follow-up assays to identify non-specific inhibitors. C1, heparin and R1 peptide, which blocks the interaction between AMA1 and RON2 (Harris et al., 2005; Richard et al., 2010), were also tested at multiple concentrations in the Nluc invasion assay which produced dose–response curves from which we could derive the half maximal effective concentration ($EC_{50}$) for egress and invasion (Supplementary Fig. S1). It should be noted that egress inhibitors, similar to C1, also inhibit invasion in this assay because the merozoites are unable to escape the iRBC (Fig. 1A).

### 3.2. A screen of the Pathogen Box compounds reveals many egress and invasion inhibitory compounds

The Pathogen Box compounds were screened at 2 μM for invasion and egress inhibition using the Nluc invasion assay. Based on control compound activity in the Z-factor assays, cut-offs for positive hits of egress inhibition were set at reducing egress to <60% and cut-offs for positive hits of invasion inhibition were set at reducing invasion to <10% (assuming vehicle control has 100% egress/invasion rates). From the screen, we found 15 compounds that reduced egress to <60% and 36 compounds that reduced invasion to <10% when normalised to DMSO at 100% (Fig. 1C and Supplementary Table S1). The hits from the Nluc screen then underwent a compound triaging process to identify compounds that were to be investigated further (Tables 1 and 2). Of the 15 compounds that inhibited egress, MMV688274 was removed since a counter screen performed with parasite lysate indicated the com-

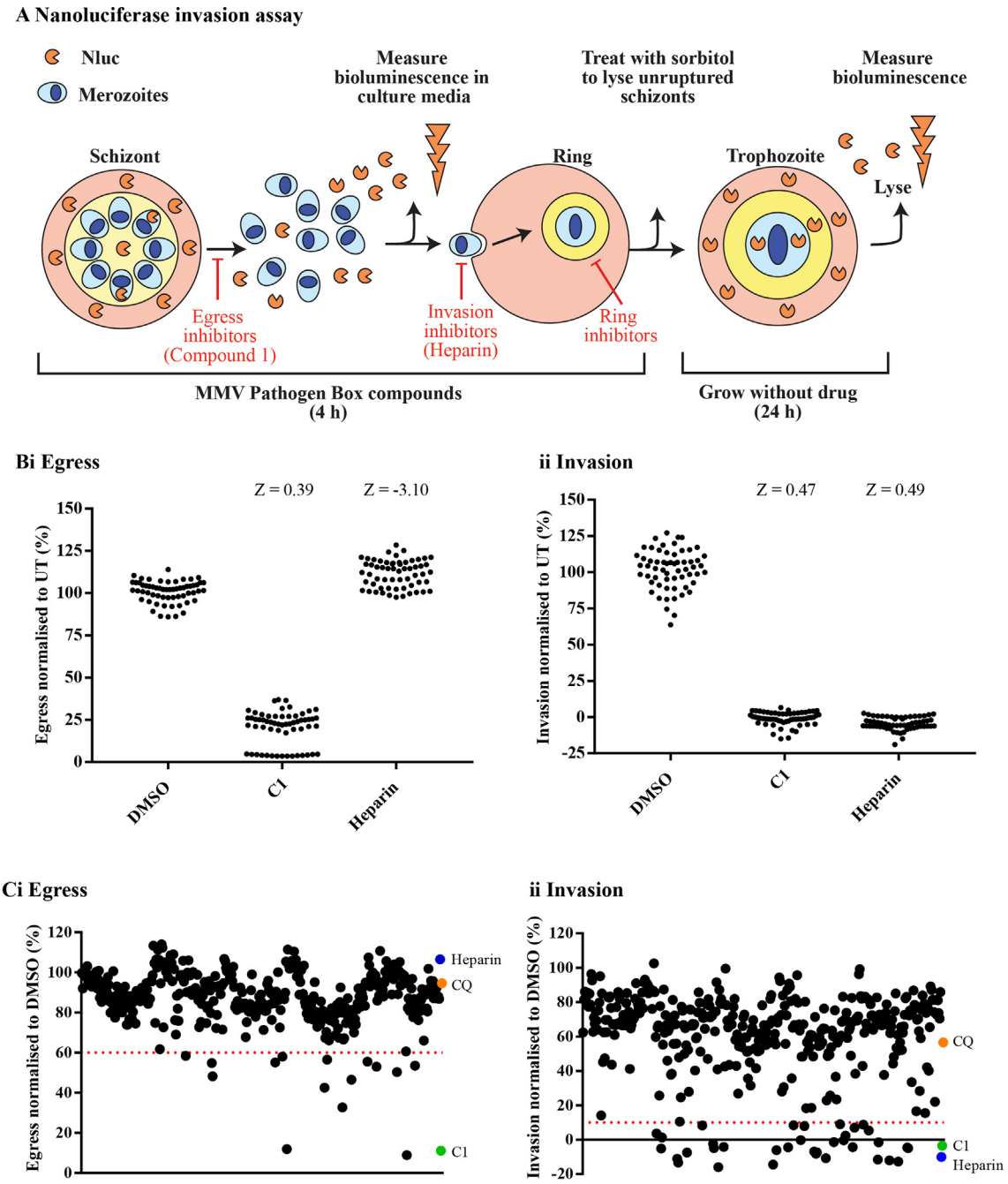


**Fig. 1.** *Plasmodium falciparum* blood stage parasites expressing an exported nanoluciferase reporter protein enables the quantification of egress and invasion and identified inhibitors of these processes in the Medicines for Malaria Venture Pathogen Box. (A) Schematic of the nanoluciferase (Nluc) invasion assay set-up whereby purified late schizonts expressing an exported Nluc were treated with compounds for 4 h. Egress inhibitors, such as Compound 1 (C1), prevent release of Nluc which was detected when the bioluminescence of the growth medium was measured after 4 h incubation. The infected red blood cells (RBCs) were then treated with 5% sorbitol to lyse schizonts, leaving newly infected ring-stage parasites behind. The ring-stage parasites were grown until trophozoites when they were lysed and their total Nluc levels measured to infer the degree of invasion. The invasion inhibitor, heparin, was used as a control compound. (B) Egress (i) and invasion (ii) of Nluc parasites following a 4 h treatment with compound vehicle DMSO, C1 or heparin that were used at concentrations of 0.02%, 4 μM and 100 μg/mL, respectively. (i) The Z-factor of 0.39 for C1 demonstrates a moderate separation band between positive and negative controls. (ii) For parasite invasion, both C1 and heparin were used as positive controls which was reflected in their Z-factors of 0.47 and 0.49, respectively. Values have been normalised and expressed as a percentage of untreated (UT) parasites. Sixty replicates were performed for each condition over three independent experiments. Z indicates Z-factor. (C) Using the Nluc egress/invasion assay, the Pathogen Box compounds were screened at 2 μM and it was found that 15 compounds reduced egress rate <60% (i) and 36 compounds reduced invasion rate <10% (ii). All values have been normalised to compound vehicle DMSO. Each dot represents the mean of a compound from three biological replicates. Dotted lines indicate cut-off values of 60% and 10% for egress and invasion inhibition, respectively. Positive control compounds, heparin and C1, were used at 100 μg/mL and 4 μM, respectively. Chloroquine (CQ) was included as a negative control at 75 nM and DMSO vehicle control was used at 0.02%.

pound inhibited Nluc activity (Supplementary Fig. S2, Table 1). Due to the design of the Nluc invasion assay, inhibitors of early ring-stage parasites (0–4 h post invasion) could be exposed to the parasites for up to 4 h, resulting in false positives for invasion inhibition (Fig. 1A). As such, compounds were tested for early ring stage growth inhibition activity and this resulted in the removal of one of the egress hit compounds, MMV667494, leaving a remaining 13 compounds targeting egress (astericks, Fig. 2A, Table 1).

**Table 1**
A nanoluciferase (Nluc) screen identified 15 Pathogen Box compounds as egress hits of *Plasmodium falciparum*.

| ID | Disease set | Egress[a] (S.D.) (%) | Invasion[a] (S.D.) (%) | Nluc activity[b] (S.D.)(%) | $EC_{50}$ growth [c] (μM) | Ring growth[d] (S.D.) (%) | Possible MoA[e] | Egress $EC_{50}$[f] (C.I.) (μM) | Invasion $EC_{50}$[f] (C.I.) (μM) |
|---|---|---|---|---|---|---|---|---|---|
| MMV020520 | MALARIA | 58.4 (31.2) | -7.5 (11.6) | 75.8 (15.1) | 1.08* | 89.8 (16.5) | PfATP4[1] | N.D. | N.D. |
| MMV006239 | MALARIA | 54.9 (22.4) | -2.5 (9.3) | 113.1 (14.1) | 0.51* | 81.7 (10.9) | PfATP4[1] | N.D. | N.D. |
| MMV000858 | MALARIA | 48.2 (18.4) | -4.9 (9.2) | 112.2 (12.2) | 1.20* | 68.4 (20.8) | PfATP4[1] | N.D. | N.D. |
| MMV687807 | TUBERC-ULOSIS | 55.2 (5.7) | -6.0 (4.8) | 91.7 (15.1) | None[#] | N.D | | N.D. | N.D. |
| MMV687273 | TUBERC-ULOSIS | 58.0 (23.8) | 30.5 (55.6) | 97.9 (14.4) | None[#] | N.D | | N.D. | N.D. |
| MMV688703 | TOXOPL-ASMOSIS | 12.0 (3.6) | -4.5 (5.1) | 92.5 (20.4) | 3.16[#] | 36.6 (23.0) | PKG[2] | N.D. | N.D. |
| MMV020081 | MALARIA | 42.6 (9.3) | -10.7 (9.2) | 96.8 (7.2) | 0.24* | 62.1 (14.8) | PfATP4[1] | N.D. | N.D. |
| MMV688274 | KINETO-PLASTIDS | 56.5 (36.1) | 50.6 (11.0) | 23.0 (3.8) | None[#] | N.D | | N.D. | N.D. |
| MMV011765 | MALARIA | 32.7 (4.2) | -0.4 (7.3) | 102.7 (3.7) | 0.27* | 75.8 (6.4) | | 0.86 (0.62-1.31) | 0.14 (0.10-0.19) |
| MMV001059 | MALARIA | 46.6 (18.2) | -4.3 (9.1) | 102.8 (3.4) | 1.09* | 101.7 (13.6) | PfATP4[1] | N.D. | N.D. |
| MMV688980 | MALARIA | 55.5 (13.2) | 5.3 (8.8) | 102.8 (2.3) | 1.97* | 83.4 (9.2) | PfATP4[1] | N.D. | N.D. |
| MMV019993 | MALARIA | 53.0 (13.4) | -11.6 (10.6) | 97.8 (3.1) | 0.10* | 37.1 (15.6) | | 0.60 (0.40-0.82) | 0.17 (0.10-0.24) |
| MMV667494 | MALARIA | 50.4 (8.5) | -12.7 (10.5) | 78.1 (18.2) | 0.01* | -8.2 (2.4) | PfEF2[9] | N.D. | N.D. |
| MMV030734 | MALARIA | 8.9 (4.2) | -4.8 (4.7) | 77.1 (15.2) | 0.41* | 91.5 (19.2) | PfCDPK1[3] | N.D. | N.D. |
| MMV016838 | MALARIA | 53.5 (26.7) | 16.6 (8.2) | 86.5 (8.1) | 0.10* | 79.6 (8.7) | PfEF2[4g] | 2.10 (1.72-2.44) | 1.26 (0.81-4.45) |

[a]Egress and invasion data derived from Nluc invasion screen representing the mean of three biological replicates performed at 2 μM (Fig. 1c).
[b]Nluc activity values represent the mean of two biological replicates in a counter screen performed at 10 μM to identify inhibitors of Nluc (Supplementary Fig. S2).
[c]$EC_{50}$ for growth data derived from Medicines for Malaria Venture (MMV; *) or Duffy et al. (2017) (#).
[d]Ring growth values demonstrate the mean of three biological replicates performed at 2 μM which identified compounds that inhibit early ring-stage parasite growth (Fig. 2).
[e]Possible mechanisms of action (MoA) (Dennis et al., 2018[1]; Zhang et al., 2006[2]; Crowther et al., 2016[3], Baragaña et al., 2015[4]; Baragaña et al., 2016[9]).
[f]$EC_{50}$ for invasion and egress determined by Nluc invasion assay. C.I., 95% confidence intervals for $EC_{50}$ values Supplementary Fig. S4.
[g]MMV0168383 was not eliminated as a PfEF2 inhibitor as it did not demonstrate early ring-stage inhibition.
Grey shading represents hits eliminated in the compound triaging process whilst compounds highlighted in yellow were sourced to study further.
N.D., not determined.

Since we were interested in studying compounds with novel egress targets, we further triaged our list of egress inhibitors to remove compounds with known targets and mechanisms of action. One of these was compound MMV688703 which was found to be structurally identical to C1 and included in the Pathogen Box as it targeted *T. gondii* PKG (Table 1) (Zhang et al., 2006). MMV030734 was also excluded since it acted upon *P. falciparum* CDPK1 (PfCDPK1) (Crowther et al., 2016), known to be involved in microneme secretion and activation of the actin-myosin motor (Table 1) (Bansal et al., 2013; Green et al., 2016). Six compounds which likely target PfATP4 were also removed since PfATP4 is involved in the efflux of excess $Na^+$ from the parasite's cytoplasm and is therefore unlikely to be directly involved in egress or invasion which we confirmed using a purified merozoite invasion assay with the known PfATP4 inhibitor, cipargamin (Table 1, Supplementary Fig. S3A) (Spillman and Kirk, 2015; Dennis et al., 2018). MMV016838 was found to be the parent compound of an antimalarial in clinical development, M5717, that targets elongation factor 2 (PfEF2) (Baragaña et al., 2015; Ashley and Phyo, 2018). However, as MMV016838 did not inhibit ring stage parasites similar to other PfEF2 inhibitors in the Pathogen Box that were hits in our screen (MMV667494 and MMV634140 (Baragaña et al., 2016)), this compound was not removed. Two additional compounds from the tuberculosis disease set were also excluded because they exhibited no antimalarial activity in the *P. falciparum* blood stage that had been previously performed by Duffy et al. (2017) (Table 1). This left three compounds, MMV011765, MMV016838 and MMV019993 of which we were able to obtain additional quantities of the first two compounds from commercial sources and MMV to further study.

Of the 36 compounds which reduced invasion to <10%, 12 of these were also inhibitors of egress and were subsequently removed, leaving a remaining 24 invasion-specific inhibitory compounds (Table 2). Two reference compounds (mefloquine (MMV000016) and pentamidine (MMV000062)) were also excluded. The invasion hits were also tested for their early ring

**Table 2**
A nanoluciferase (Nluc) screen revealed 24 Pathogen Box compounds as invasion-specific hits of *Plasmodium falciparum*.

| ID | Disease set | Invasion[a] (S.D.) (%) | Nluc activity[b] (S.D.) (%) | $EC_{50}$ growth[c] (μM) | Ring growth[d] (S.D.) (%) | Possible MoA[e] | Invasion $EC_{50}$[f] (C.I.) (μM) |
|---|---|---|---|---|---|---|---|
| MMV000062 | REF. (PENTAMIDINE) | 3.6 (10.6) | 96.4 (6.1) | N/A | N.D. | | N.D. |
| MMV020623 | MALARIA | -5.1 (11.4) | 90.1 (6.9) | 0.94* | 71.0 (3.6) | PfATP4[1] | N.D. |
| MMV020512 | MALARIA | 1.2 (10.8) | 94.1 (8.4) | 0.48* | 47.6 (4.3) | | 1.15 (0.30-UND) |
| MMV020136 | MALARIA | -11.1 (10.6) | 91.8 (30.8) | 1.10* | 89.3 (5.6) | PfATP4[1] | N.D. |
| MMV020710 | MALARIA | -13.3 (10.2) | 81.9 (22.6) | 0.24* | 75.8 (9.2) | PfATP4[1] | N.D. |
| MMV019721 | MALARIA | 10.6 (13.3) | 90.9 (22.1) | 0.50* | 53.3 (26.1) | | 1.47 (0.91-7.38) |
| MMV637229 | TRICHURIASIS | 8.3 (9.5) | 105.7 (17.3) | 2.20# | 81.6 (12.7) | | 0.49 (0.38-0.63) |
| MMV000016 | REF. (MEFLOQUINE) | -15.9 (11.1) | 105.5 (16.3) | N/A | N.D. | | N.D. |
| MMV020391 | MALARIA | -4.2 (11.7) | 101.9 (19.6) | 0.93* | 105.1 (4.9) | PfATP4[1] | N.D. |
| MMV023969 | TUBERCULOSIS | -14.5 (8.7) | 100.2 (10.2) | 0.59# | -7.2 (2.2) | | N.D. |
| MMV024311 | TUBERCULOSIS | 8.4 (14.4) | 104.1 (20.6) | 0.75# | -1.6 (3.2) | | N.D. |
| MMV010576 | MALARIA | -0.3 (13.7) | 93.8 (5.1) | 0.10* | 42.3 (6.2) | PI4K[5,6] | N.D. |
| MMV688362 | KINETOPLASTIDS | 7.9 (10.9) | 98.1 (5.7) | 0.59# | 12.2 (5.3) | DNA binding agent[8,10] | N.D. |
| MMV024035 | MALARIA | -6.8 (9.6) | 87.4 (15.2) | 0.57* | -3.0 (5.2) | | N.D. |
| MMV020291 | MALARIA | -8.2 (9.2) | 100.6 (8.8) | 0.91* | 95.6 (12.9) | | 0.38 (UND-0.45) |
| MMV006833 | MALARIA | -7.3 (7.2) | 95.3 (12.4) | 0.30* | 99.3 (12.5) | | 0.17 (0.06-0.23) |
| MMV023233 | MALARIA | -1.4 (4.6) | 104.5 (0.01) | 0.16* | -0.7 (5.4) | | N.D. |
| MMV688279 | KINETOPLASTIDS | 9.0 (11.2) | 88.8 (19.5) | 0.32# | 54.5 (2.4) | | 0.61 (UND) |
| MMV085499 | MALARIA | 2.3 (10.5) | 90.1 (4.0) | 0.10* | 55.5 (10.8) | PI4K[7] | N.D. |
| MMV676877 | MALARIA | 7.1 (4.6) | 91.2 (1.0) | 0.66* | 91.4 (5.1) | | 1.16 (0.65-54.37) |
| MMV676881[T] | MALARIA | 8.8 (5.9) | 98.4 (4.7) | 0.90* | 75.6 (13.1) | Cysteine proteases[11,12] | 0.19 (0.10-0.30) |
| MMV687794 | MALARIA | -1.5 (9.7) | 86.9 (2.6) | 0.3* | 96.2 (17.4) | | 0.34 (0.23-0.49) |
| MMV671636 | ONCHOCERCIASIS | -12.0 (8.6) | 90.3 (20.2) | 1.01# | 33.4 (31.5) | Mitochondria[8] | N.D. |
| MMV634140 | MALARIA | -4.6 (10.9) | 90.1 (10.6) | 0.10* | 16.8 (7.05) | PfEF2[9] | N.D. |

[a]Invasion data derived from Nluc invasion screen representing the mean of three biological replicates performed at 2 μM (Fig. 1c).
[b]Nluc activity values represent the mean of two biological replicates performed at 10 μM in a counter screen to identify inhibitors of Nluc (Supplementary Fig. S2).
[c]$EC_{50}$ for growth data derived from Medicines for Malaria Venture (MMV; *) or Duffy et al. (2017) (#).
[d]Ring growth values demonstrate the mean of three biological replicates performed at 2 μM which identified compounds that inhibit early ring parasite growth (Fig. 2).
[e]Possible mechanisms of action (MoA) (Dennis et al., 2018[1]; Younis et al., 2012[5]; Paquet et al., 2017[6]; Le Manach et al., 2016[7]; Duffy et al., 2017[8]; Baragaña et al., 2016[9]; Rodríguez et al., 2008[10]; Mott et al., 2010[11]; Veale, 2019[12]).

[f]$EC_{50}$ for invasion determined by Nluc invasion assay. C.I., 95% confidence intervals for $EC_{50}$ values Supplementary Fig. S4.
[T]MMV676881 identified in the screen as invasion inhibitor was found to be an egress inhibitor upon further characterisation.
Grey shading represents hits eliminated in the compound triaging process whilst compounds highlighted in yellow were sourced to study further.
N.D., not determined; N/A, not applicable; UND, undefined.

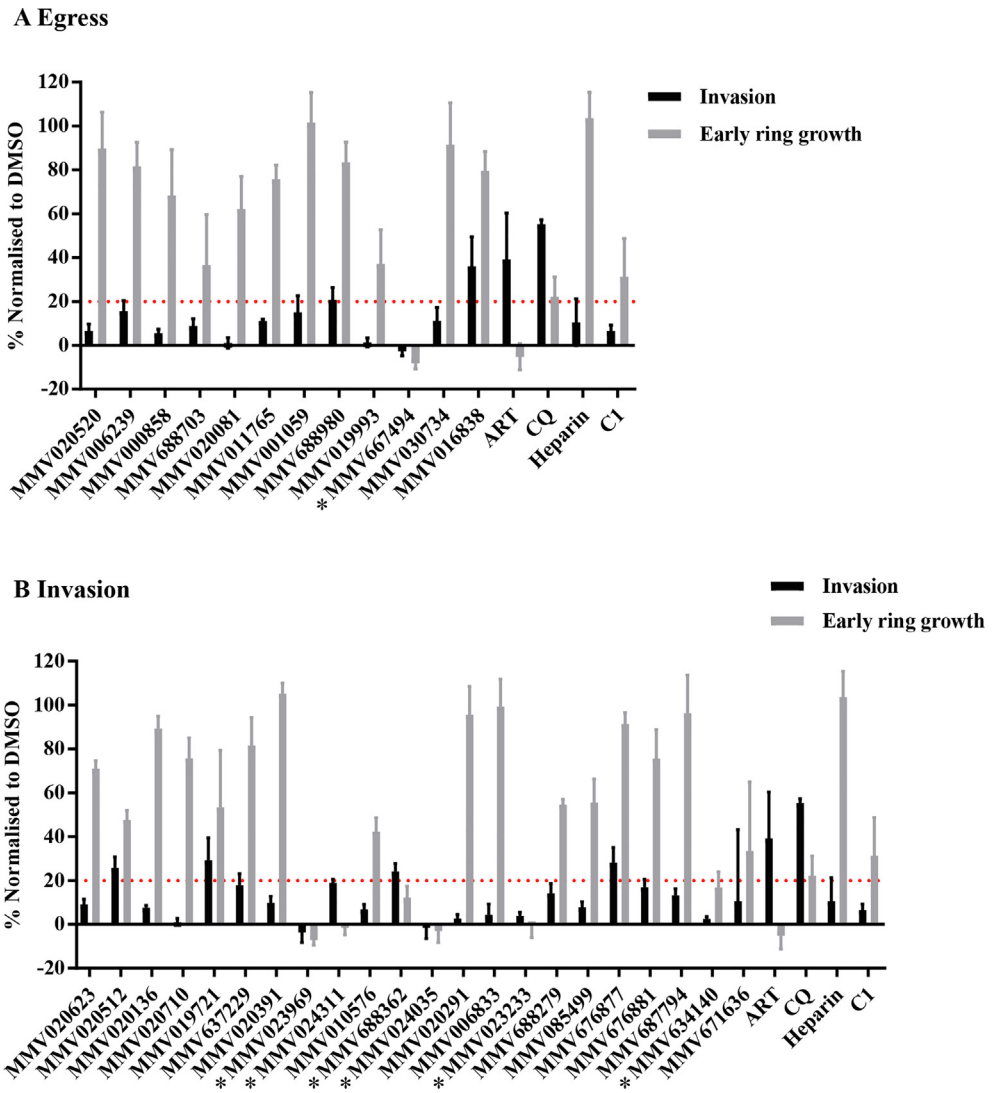


**Fig. 2.** Multiple egress and invasion inhibitors also target the early *Plasmodium falciparum* ring stage of intracellular growth. The lead compounds from the egress screen (A) and the invasion screen (B) were assessed for their ability to inhibit early ring parasites (4–8 h post invasion) at a concentration of 2 μM in the Nluc invasion assay. One compound from the egress screen and six compounds from the invasion screen potently inhibited ring stage parasites (*). Artemisinin (ART) was included as a positive control for ring stage inhibition at a concentration of 25 nM, and negative controls were chloroquine (CQ), compound 1 (C1) and heparin which were used at concentrations of 75 nM, 4 μM and 100 μg/mL, respectively. Values were normalised to DMSO at a concentration of 0.02%. Dotted line indicates 20% cut-off for early ring stage inhibitors. Error bars represent the S.D. of three biological replicates.

stage growth inhibition activity and this resulted in the removal of six compounds (MMV023969, MMV024311, MMV688362, MMV024035, MMV023233, MMV634140) (asterisks, Fig. 2B and Table 2). Compounds targeting PI4K, the mitochondrial cytochrome bc1 complex, DNA machinery, PfEF2 and PfATP4 were removed since their protein targets have likely non-invasion related roles (Table 2) (Rodríguez et al., 2008; Younis et al., 2012; Baragaña et al., 2016; Le Manach et al., 2016; Duffy et al., 2017; Paquet et al., 2017; Dennis et al., 2018). This left nine compounds targeting invasion which we were able to obtain supplementary amounts of from commercial sources or MMV to conduct phenotypic analyses.

### 3.3. Categorising egress and invasion inhibitory compounds

To identify the phenotypes of these invasion and egress inhibitors, Giemsa-stained blood smears were examined from schizonts that had been treated for 4 h with 2 μM of the hit compounds (Fig. 3, Supplementary Table S2). It was found that the egress

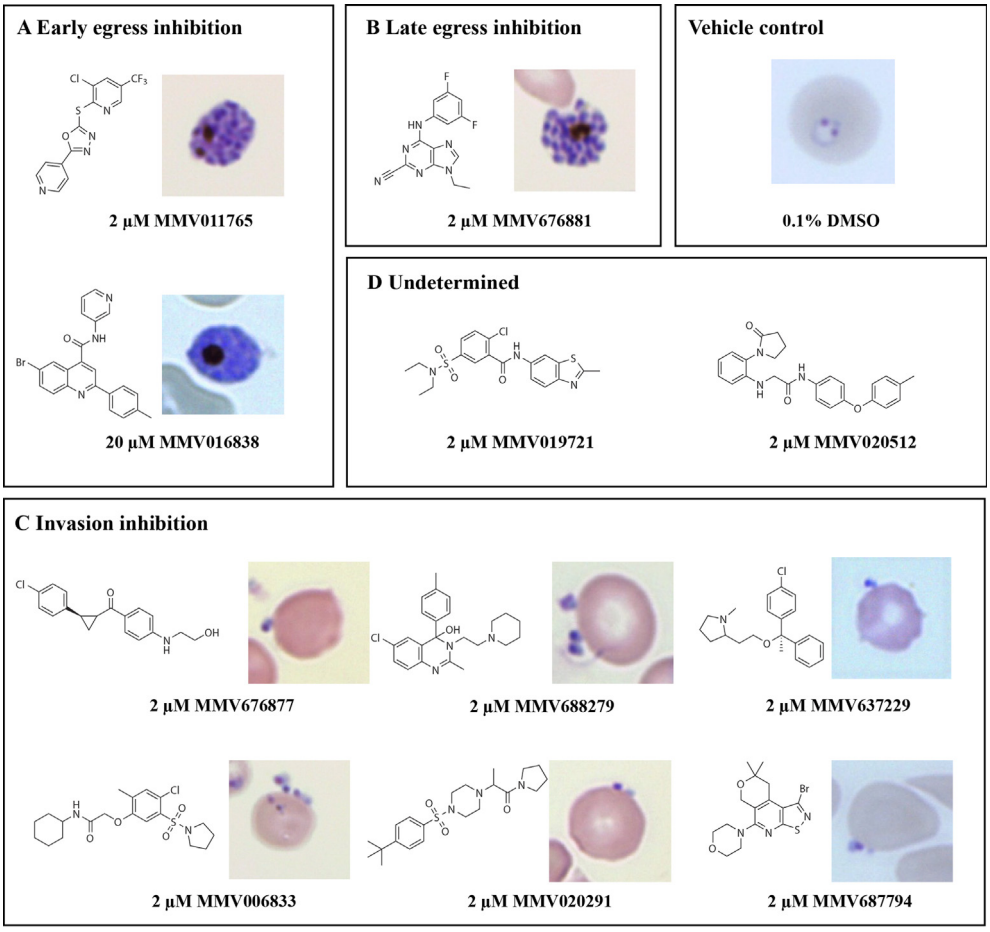


**Fig. 3.** Giemsa stained thin blood smears of *Plasmodium falciparum* parasites following treatment with lead egress and invasion-inhibitory compounds. Depicted are two early egress inhibitory compounds, one late egress inhibitor and six compounds with invasion inhibitory activity. Giemsa-stained smears following a 4 h treatment of schizonts with 2 µM of Pathogen Box compounds (or 20 µM, MMV016838) were used to categorise the lead compounds into either early egress inhibitors (A), late egress inhibitors (B), invasion inhibitors (C) or undetermined (D). Vehicle control indicates schizonts treated with 0.1% DMSO.

inhibitor, MMV011765, halted schizont maturation at the point when the merozoites had formed but had not yet physically separated possibly due to an intact PVM (Fig. 3A). The egress inhibitor, MMV016838 did not appear to inhibit egress or invasion at 2 µM compared with vehicle control. Therefore, the concentration was increased to 20 µM (10 × $EC_{50}$ of egress, Supplementary Fig. S4Ai) upon which a similar inhibition of schizont/merozoite maturation phenotype to MMV011765 and C1 was observed (Fig. 3A). Based on the Nluc screen, MMV676881 was predicted to be an invasion inhibitor, however Giemsa stained smears indicated that MMV676881 prevented merozoite egress, probably after breakdown of the PVM but not the RBC membrane since the merozoites appeared physically separated within the schizont (Fig. 3B).

Of the remaining eight invasion inhibitors identified in the screen, six (MMV676877, MMV006833, MMV637229, MMV020291, MMV688279, MMV687794) demonstrated a degree of invasion inhibitory activity by Giemsa stained smears since fewer rings were observed than in the DMSO vehicle control (Supplementary Table S2). In agreement with this, there were more merozoites counted (free and collocated with RBCs) in proportion to DMSO, (Fig. 3C, Supplementary Table S2). The remaining two compounds identified as invasion inhibitors from the screen (MMV019721 and MMV020512) had inconclusive phenotypes whereby MMV020512 treatment did not increase the proportion of merozoite or decrease the proportion of schizonts, relative to DMSO (Supplementary Table S2). MMV019721 did increase the proportion of schizonts relative to DMSO, however a number of ring stage parasites were also present, making it unclear how the compound was affecting egress and/or invasion (Fig. 3D).

### *3.4. Egress inhibitors function at two stages of schizont maturation and do not specifically affect merozoite invasion of RBCs*

To further characterise the egress inhibitors, live schizonts were examined under culture conditions by brightfield microscopy after 4 h of drug treatment. MMV011765 and MMV016838 treatment revealed they were similar to C1-arrested schizonts where the merozoites were indistinct from each other, possibly because they were spatially confined with intact PVM and RBC compartments (Fig. 4Ai). To test if this inhibition was reversible, schizonts expressing Nluc were treated with C1, MMV011765 or MMV016838 for 2 h to arrest egress which was confirmed due to reduced Nluc activity in the growth medium relative to a DMSO control (Fig. 4Aii). To measure reversibility, the compounds were washed out and egress was allowed to proceed for a further 4 h. Nluc activity in the growth medium indicated egress had resumed for the reversible inhibitor, C1, and MMV016838 but not for MMV011765. This indicates that the latter is an irreversible egress inhibitor, either by irreversibly binding to its target protein to disrupt function or by being resistant to wash-out methods (Fig. 4Aii).

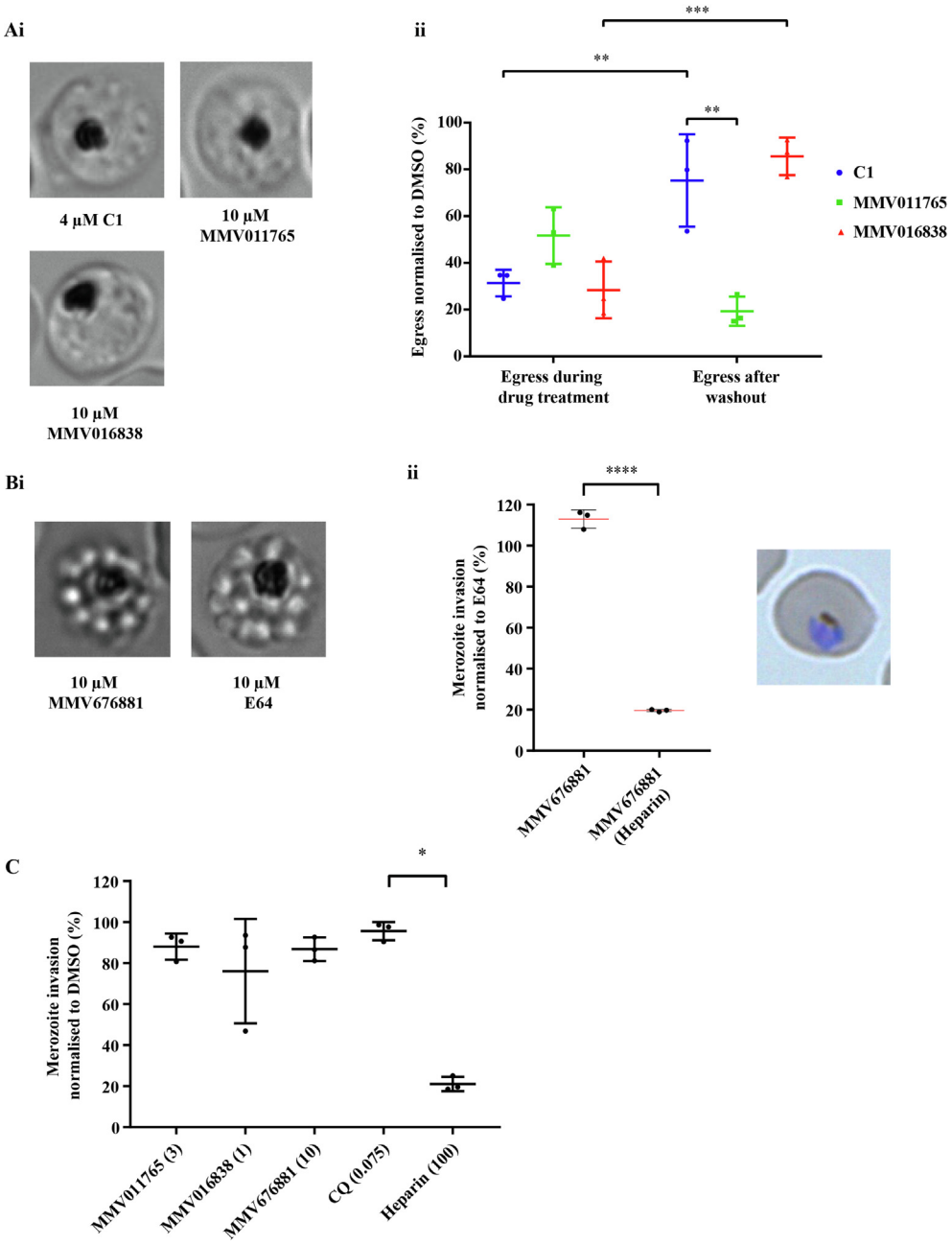


**Fig. 4.** Treatment of *Plasmodium falciparum* schizonts with egress inhibitors reveals some compounds are reversible and/or do not specifically inhibit invasion of purified merozoites. (A) (i) Brightfield microscopy reveals treatment of schizonts with 10 μM MMV011765 and MMV016838 blocks the maturation and separation of merozoites similar to treatment with 4 μM Compound 1 (C1). (ii) Measurement of egress during and after the removal of inhibitory compounds as determined by the release of nanoluciferase (Nluc) into the growth medium indicates MMV011765 is an irreversible inhibitor whilst MMV016838 is a reversible inhibitor, similar to C1. Values have been normalised to 0.1% DMSO with concentrations of Medicines for Malaria Venture compounds at 10 μM and C1 at 4 μM. (B) (i) Live cell microscopy demonstrates that MMV676881 prevents the release of merozoites, similarly to the protease inhibitor E64 by producing red blood cell (RBC) membrane trapped merozoites. Single frames of videos are shown in (i) (Supplementary Videos S1, S2) after a 4 h treatment of schizonts with 10 μM MMV676881 and 10 μM E64. (ii) Mechanical rupture of RBC membranes after 4 h treatment with 10 μM MMV676881 and 10 μM E64 demonstrated the merozoites were viable and invasion competent with exposure to MMV676881 resulting in a similar degree of invasion as E64-treatment as determined by measurement of Nluc activity 24 h later. Control compound heparin inhibited merozoite invasion of MMV676881 treated schizonts. A Giemsa stained smear of a trophozoite at 24 h post invasion after MMV676881 schizont treatment showing that merozoites invaded and progressed to trophozoites normally. All values have been normalised to 10 μM E64. (C) Merozoite invasion assays demonstrate MMV011765, MMV016838 and MMV676881 at 10 × $EC_{50}$ for growth (concentrations in μM specified in brackets or μg/mL for heparin) were specific for egress inhibition with merozoite invasion remaining relatively unaffected. No significant difference between the Medicines for Malaria Venture compounds and chloroquine (CQ) was seen, in contrast to heparin. Values have been normalised to 0.1% DMSO. Statistical analysis for (A) (ii) was performed via two-way ANOVA; (B) (ii), unpaired *t* test; (C), one-way ANOVA using GraphPad Prism. $^{*}P < 0.05$, $^{**}P < 0.01$, $^{***}P < 0.001$ and $^{****}P < 0.0001$. No bar indicates not significant. Error bars represent the S.D. of three biological replicates.

MMV0168383 treated schizonts also had some reduction in merozoite invasion after egress had resumed (Supplementary Fig. S5).

Next, schizonts were treated with the later acting MMV676881 and when visualised by brightfield microscopy, RBCM trapped merozoites were observed, resembling treatment with the cysteine protease inhibitor, E64 (Fig. 4Bi, Supplementary Videos S1 and S2). It should be noted that E64 does not prevent Nluc release in the Nluc invasion assay, similar to MMV676881 (Supplementary Fig. S3B). To further support MMV676881 acting as an E64-like inhibitor, a merozoite viability assay was performed whereby puri-

fied schizonts were treated with either MMV676881 or E64 to induce RBCM trapped merozoites, and mechanically broken open to release merozoites to allow invasion of new RBCs. A negative control containing heparin was also included to block invasion. Ring-stage parasites were grown for 24 h and the degree of invasion was inferred by measuring the Nluc activity of the whole culture. The Nluc activity of trophozoites treated with MMV676881 at schizonts in the previous cycle was, on average, 108% of those treated with E64, with heparin reducing invasion to 20% (Fig. 4Bii, $P < 0.0001$), demonstrating that both MMV676881 and E64 block merozoite egress but do not affect the merozoites ability to invade RBCs. This strengthens support for MMV676881 acting similarly to an E64-like egress inhibitor by preventing breakdown of RBC membranes, without affecting merozoite viability.

The three egress inhibitors, MMV011765, MMV016838 and MMV676881, were also tested for their ability to specifically inhibit merozoite invasion in invasion assays with purified merozoites (Boyle et al., 2010b; Wilson et al., 2013, 2015). Briefly, purified schizonts were treated with E64 until the formation of RBCM trapped merozoites, then mechanically ruptured to release the merozoites. The merozoites were rapidly added to fresh RBCs in the presence of 10 × $EC_{50}$ of the compounds and left to invade the RBCs at 37 °C for 30 min. The compounds were then washed out of the new ring stage parasites and cultured for a further 24 h with quantification of invasion performed by measuring Nluc activity present in trophozoite iRBCs. This revealed that MMV011765, MMV016838 and MMV676881 did not affect merozoite invasion of RBCs, with no differences observed between the egress inhibitors and the antimalarial, chloroquine, which does not inhibit invasion. In contrast, the control compound heparin dramatically reduced the degree of RBC invasion (Fig. 4C). Taken together, these findings indicate that MMV011765, MMV016838 and MMV676881 are inhibitors of merozoite egress at early and late stages of schizont maturation and do not specifically inhibit merozoite invasion of RBCs.

### 3.5. Two inhibitors, MMV020291 and MMV006833, appear to specifically block merozoite entry into RBCs

The eight compounds (MMV676877, MMV006833, MMV637229, MMV020291, MMV688279, MMV687794, MMV019721 and MMV020512) that were predicted to inhibit invasion from the Nluc screen (six of which displayed invasion inhibitory effects by morphological examination of Giemsa stained smears) were tested for a direct inhibition of merozoite invasion by performing purified merozoite invasion assays as described above. This revealed that only one of the compounds, MMV020291, could directly block merozoite invasion to a similar degree to that of the heparin control (Fig. 5A). MMV637229, MMV006833 and MMV020512 had an intermediate effect, whereas the other compounds, MMV676877, MMV019721, MMV687794 and MMV688279 caused negligible invasion inhibition, similar to chloroquine (Fig. 5A).

We hypothesised that the intermediate invasion inhibitory compounds may be exerting their invasion inhibitory effects by causing general growth defects during the window of merozoite egress and/or invasion. We ascertained this by measuring the effects of compounds on other stages in the asexual lifecycle. Whilst activity against ring-stage parasites (4–8 h post invasion), was a criterion for elimination in compound triaging from the screen, it was possible that these compounds may be active at other stages. Therefore, trophozoites (~24 h post invasion) were exposed to the lead compounds at 10 × $EC_{50}$ of growth for 4 h before being washed out and allowed to proceed to the following cycle, where they were assessed for growth via Nluc activity. It was found that five of the invasion inhibitory compounds (MMV676877, MMV637229, MMV688279, MMV019721 and MMV020512) and one of the egress inhibitors (MMV016838), decreased trophozoite growth with invasion inhibitors MMV637229 and MMV688279 causing a significant reduction in growth compared with control compound heparin (Fig. 5B). This

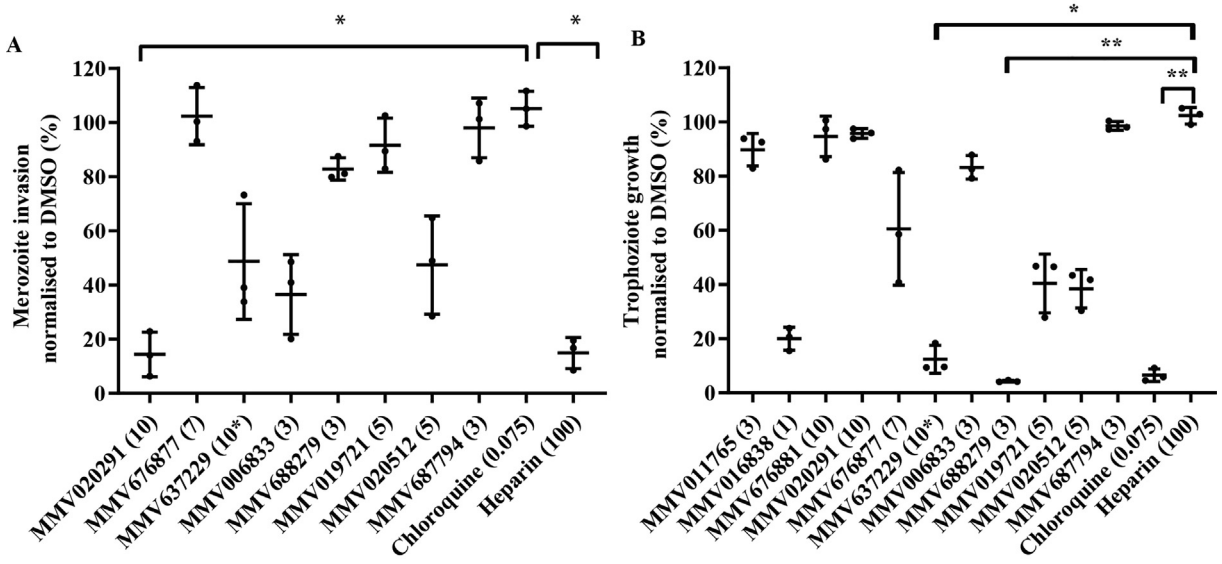


**Fig. 5.** MMV020291 is the most specific invasion inhibitory compound. (A) *Plasmodium falciparum* merozoite invasion assays demonstrates one of the eight invasion inhibitors identified from the screen, MMV020291, is the only compound to directly block merozoite invasion into red blood cells (RBCs) to a similar degree as heparin. MMV637229, MMV006833 and MMV020512 induce intermediate invasion inhibitory effects whereas the remaining compounds have little effect. (B) Growth of trophozoite stage parasites after exposure to the lead compounds for 4 h demonstrates that multiple compounds (MMV688279, MMV637229, MMV016838) reduce trophozoite growth with MMV688279, causing significant growth reduction when compared with the control compound, heparin. Pathogen Box compounds were tested at concentrations (μM), specified in brackets which were equivalent to 10 × $EC_{50}$ of growth (or 5 × $EC_{50}$ for MMV637229*) or μg/mL for heparin. Values have been normalised to 0.1% DMSO. Error bars represent the S.D. of three biological replicates. Statistical analysis performed via one-way ANOVA in GraphPad Prism between chloroquine (A) and heparin (B) and Pathogen Box compounds. *$P < 0.05$, **$P < 0.01$. No bar indicates not significant.

corroborated the results from the purified merozoite invasion assay which demonstrated that not all of these compounds specifically block merozoite invasion, thereby alluding to inhibitors that affect general processes in the parasite that may be required at the time of invasion. As MMV020291 and MMV006833 did not inhibit trophozoite growth and demonstrated invasion inhibitory activity in the purified merozoite invasion assay, we next investigated which stage of invasion was being blocked by these compounds.

### *3.6. Live cell imaging of the two lead invasion inhibitors, MMV020291 and MMV006833, indicate MMV020291 blocks successful merozoite invasion of RBCs and MMV006833 slows down the invasion process, arresting ring formation*

In order to gain an understanding of which stage of invasion might be affected by MMV020291 and MMV006833, we assessed the kinetics and physical morphology of *P. falciparum* invasion of RBCs by live cell microscopy using methods that had been previously developed (Weiss et al., 2015) (Supplementary Videos S3–S5). For consistency we used the same Hyp1-Nluc 3D7 parasite line as the invasion screen, with 0.1% DMSO as the vehicle control where we filmed and analysed 10, 11 and 12 egress events for MMV020291, MMV006833 and DMSO treatment, respectively. After each schizont rupture, in the presence of 10 μM MMV020291 or 2 μM MMV006833 (~10 × $EC_{50}$), the number of merozoites which adhered to neighbouring RBCs for ≥2 s per egress was comparable to DMSO (DMSO mean: 24.0 merozoites, MMV020291 mean: 25.3 merozoites, MMV006833 mean: 25.3 merozoites) (Supplementary Fig. S6A). This indicated the compounds had not reduced the initial adhesiveness of the merozoites (note that merozoites may contact more than one RBC). Merozoites that maintain contact with their target RBCs then typically proceed to deform the surface of the RBC they attempt to invade. The time of initial merozoite contact to start of RBC deformation and duration of deformation upon MMV020291 treatment was comparable to the DMSO control (Fig. 6Ai, Supplementary Fig. S6B). In contrast, MMV006833 significantly delayed the ability of the merozoite to induce RBC deformation but did not affect the duration of deformation (Fig. 6Ai, Supplementary Fig. S6B).

Next, the degree of RBC deformation caused by merozoite contact following compound treatments was scored to assess receptor-ligand interactions during early stages of *P. falciparum* invasion of RBCs where the intensity of RBC deformation is positively correlated with successful invasion (Weiss et al., 2015). Merozoite contact with no RBC deformation was scored as 'zero' and strong deformation with the merozoite wrapping the RBC around itself was scored 'three' with intermediate effects scoring 'one' and 'two' (Weiss et al., 2015). In the presence of MMV020291 there was a significant decrease in the deformation score whilst the degree of deformation remained unchanged with MMV006833 treatment (Fig. 6Aii). A further qualitative observation was that treatment with MMV020291 appeared to reduce gliding motility of the merozoites across the RBC surface (Supplementary Video S6, DMSO and Supplementary Video S7, MMV020291).

Although MMV020291 treated merozoites appeared to attempt to invade their target RBCs, none completed the invasion process to achieve complete internalisation into the RBC. This is in contrast to an average of 3.4 and 3.3 invasions per merozoite egress in the DMSO control and MMV006833 treatments, respectively (Fig. 6Aiii). Although, MMV006833 treated merozoites invaded, they took significantly longer to penetrate their RBCs than the DMSO control (14.0 s versus 10.1 s respectively, $P$ = 0.0012, Fig. 6Aiv).

Merozoite invasions typically cause their target RBCs to rapidly undergo echinocytosis, a process where they develop a stellate appearance which returns to a normal biconcave shape after several minutes, by which time the merozoite has differentiated into a ring (Gilson and Crabb, 2009; Weiss et al., 2015). Although MMV020291 treated merozoites did not successfully invade, they still triggered echinocytosis in an average of 4.0 RBCs per egress. This was not significantly different to the average 2.5 and 2.8 RBC echinocytosis events per egress in the DMSO control and MMV006833 treatment, respectively (Supplementary Fig. S6C, $P$ = 0.07 (DMSO and MMV020291)).

Even though MMV020291 and MMV006833 treatment still triggered RBC echinocytosis, the compounds greatly prolonged the echinocytosis period (903.6 and 795.8, respectively) compared with the DMSO control that saw an echinocytosis period of an average of 404.1 seconds (Fig. 6Av). Note that the echinocytosis periods for MMV compound treatments are an underestimate because the echinocytosed RBCs had often not recovered their normal shape by the end of the 20 min filming period.

After invasion was complete, merozoites began to differentiate into amoeboid, ring stage parasites several minutes later. The process started with the growth of an arm-like projection or pseudopod from the internalised merozoite before full differentiation into an amoeba. In the DMSO control, ring conversion was completed in most invasions within 1 min (Fig. 6Avi, Supplementary Video S3, black arrow), whereas ring formation appeared to be greatly slowed down or even arrested with MMV006833 treatment (mean: 803.9 s, Fig. 6Avi, $P$ < 0.0001, Supplementary Video S5, black arrows). The time taken for ring formation after MMV006833 treatment was an underestimate of the severity of the defect, since the 20 min filming period frequently ended before ring formation was complete.

After echinocytosis had commenced following MMV020291 treatment, pseudopodial protrusions began to appear on the outside of RBCs where the merozoites had failed to invade (Fig. 6B). Here, 100% of egress events and stalled invasions produced protrusions on at least one RBC, with a maximum of eight different RBCs developing protrusions after a single egress event (Fig. 6Avii). This is probably an underestimate of the pseudopod formation since many of the merozoite contacted RBCs had more than one protrusion. The formation of pseudopods from failed invasions was also occasionally observed with merozoites treated with DMSO and MMV006833, where 16.6% and 9.1% of egress events produced a single protrusion on the surface of a single RBC, respectively (Fig. 6Avii).

To gain an indication that the pseudopods formed from MMV020291 blocked invasions were equivalent to the formation of pseudopods during ring formation, we compared the duration of echinocytosis to pseudopodia formation for MMV020291 with DMSO and MMV006833 treatments. Here, no significant difference was observed (Fig. 6Aviii, DMSO mean: 324.2 s, MMV020291 mean: 261.0 s, MMV006833 mean: 332.0 s), indicating that the protrusions formed after MMV020291 treatment might emanate from merozoites that had begun to differentiate into rings on the outside of the RBCs they had failed to invade.

In order to confirm that these pseudopods observed after MMV020291 treatment were parasite-derived, rather than originating from the RBC, purified schizonts and RBCs were stained with fluorescent green and red bodipy membrane dyes, respectively. This revealed that the MMV020291 induced pseudopods were red and therefore merozoite derived, either as a result of cell lysis or aberrant differentiation into ring-like parasites at the RBC surface following invasion failure. The fluorescent green RBC dye also revealed a distinct circular or "punctate structure" at the RBC invasion site, possibly originating from failed PV formation (Fig. 6C, white arrows).

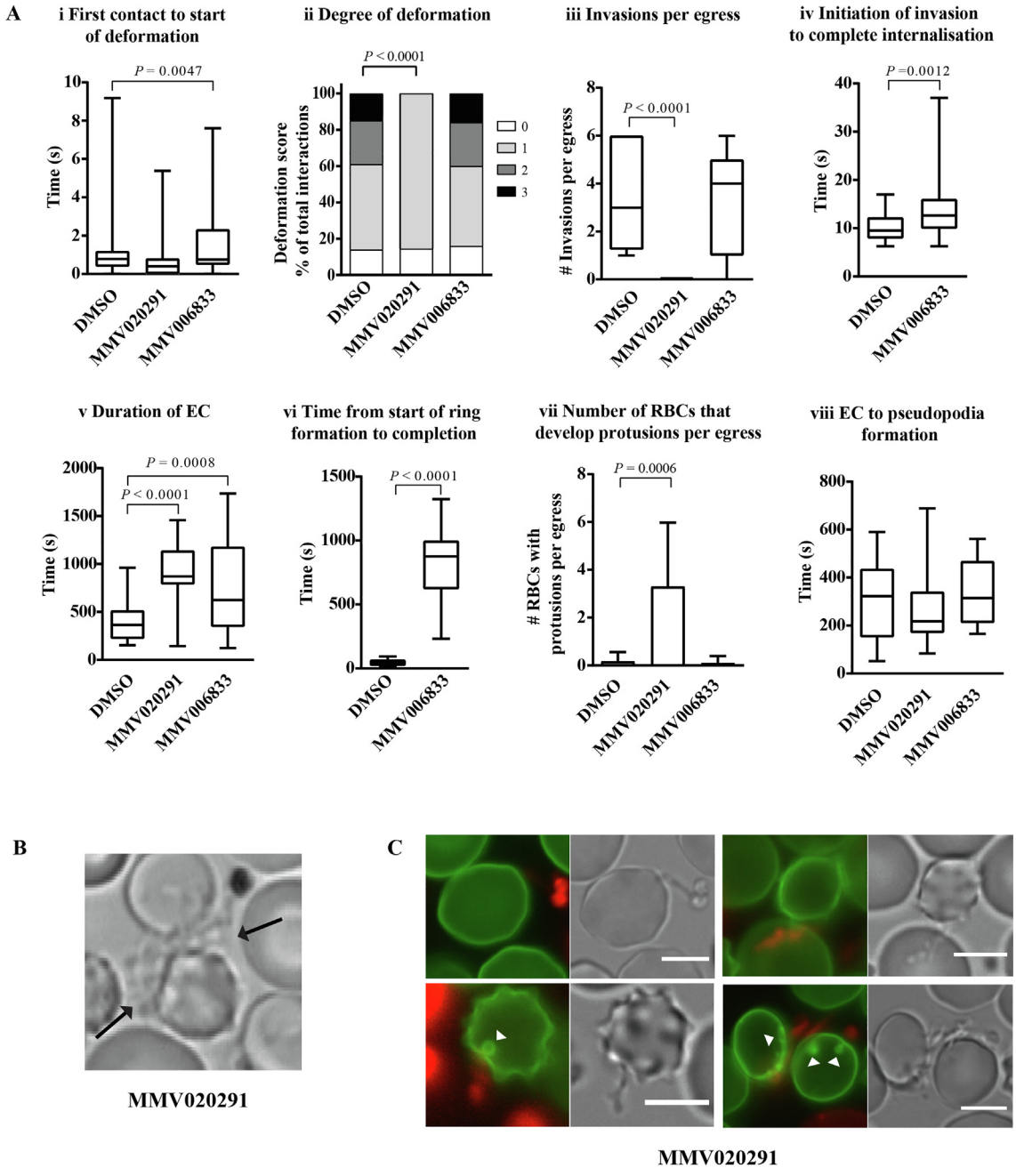


**Fig. 6.** Live cell microscopy reveals MMV020291 blocks *Plasmodium falciparum* merozoite invasion and MMV006833 significantly slows down the invasion process and arrests conversion into ring stages. (A) (i) Analysis performed on live cell microscopy videos of parasites treated with 10 μM MMV020291 and 2 μM MMV006833 demonstrated an increase in the time taken for MMV006833 treated merozoites to cause deformation in the red blood cell (RBC) membrane after first contact compared with vehicle control, 0.1% DMSO. (ii) MMV020291 treated merozoites markedly lacked the ability to deform RBC membranes compared with DMSO. (iii) MMV020291 revealed complete inhibition of merozoite invasion in contrast to DMSO and MMV006833 successful invasions. (iv) MMV006833 treated merozoites significantly increased the time taken from initialisation of the invasion event until complete internalisation within the RBC. (v) Treatment of merozoites with both invasion inhibitory lead compounds lead to significant prolonging in the duration of RBC echinocytosis. (vi) MMV006833 caused a significant increase in the time taken from the start of ring formation to completion. (vii) MMV020291 caused a significant number of protrusions to form at site of merozoite contact with target RBCs after egress events occurred. (viii) There were no differences observed between time taken from echinocytosis to pseudopodia formation for both DMSO and MMV006833 treatment after merozoite invasion, and time taken from echinocytosis to external pseudopodia formation on the RBC surface with MMV020291 treatment. (B) Frame of a live cell microscopy video showing a ruptured schizont treated with 10 μM MMV020291 and the merozoites that attempted but could not complete invasion, which formed protrusions extending from the point of contact with the RBC (black arrows) (Supplementary Video S4). (C) Brightfield and fluorescence images of failed merozoite invasions following 10 μM MMV020291 treatment. The RBCs were stained with BODIPY FL $C_{12}$- Sphingomyelin (green) and the merozoites with BODIPY TR ceramide (red) which demonstrated the protrusions were derived from merozoite material. A green "punctum" was also sometimes observed on the RBC at the site of merozoite contact (white arrow heads). Schizont rupture events (12, 10 and 11) were filmed and analysed for DMSO, MMV020291 and MMV006833 treatment, respectively. Images and videos were analysed using ImageJ. Statistical analysis were performed on GraphPad Prism using unpaired *t* tests (Ai, iii-viii) and Chi-square contingency (Aii). No bar indicates not significant. EC, echinocytosis. #. number. Scale bars indicate 5 μm.

## 4. Discussion

In this study, we have shown that by using the bioluminescent reporter protein, Nluc, it was possible to effectively screen compound libraries for inhibitors of parasite egress and invasion of RBCs in a microplate-based manner. Using this technique, we screened the MMV Pathogen Box and identified 15 compounds that inhibit parasite egress and 24 invasion-specific inhibitory compounds. We independently sourced 11 of these compounds and investigated their activity on *P. falciparum* using various growth and invasion assays, in addition to live cell microscopy.

After performing these validation assays, we grouped these compounds into one of five following categories; (1) blockers of late schizont maturation (MMV011765, MMV016838), (2) inhibitor of the breakdown of the iRBC membranes and merozoite egress (MMV676881), (3) direct blocker of merozoite invasion of RBCs (MMV020291), (4) inhibitor of the invasion process and ring development (MMV006833) and (5) general growth inhibitors that have a strong effect on invasion (MMV676877, MMV637299, MMV688279, MMV687794, MMV019721, MMV020512) (Fig. 7).

Using brightfield microscopy, the three Pathogen Box egress inhibitors induced phenotypes resembling treatment with E64 and C1, compounds that target cysteine proteases and PKG, respectively. PfPKG has been shown to be a master regulator of egress by sitting at the top of a cascade of events that culminate in merozoite release (Taylor et al., 2010; Hopp et al., 2012; Collins et al., 2013). Treatment of schizonts with MMV011765 and MMV016838 induced a developmental arrest of merozoites that was indistinct from each other, indicating an early stage of maturation was hindered, as seen in C1-treated schizonts. However, MMV011765 appears to be irreversible suggesting that this compound permanently binds to its target, prevents a time sensitive event that cannot be resumed in order to produce viable merozoites or may be retained intracellularly despite wash-out attempts. In a recent screen of the Pathogen Box for *T. gondii* inhibitors, MMV011765 was identified as one of eight compounds in the Pathogen Box with activity against *T. gondii* tachyzoites (Spalenka et al., 2018). Identifying the target of MMV011765 may provide further knowledge into the complex signalling mechanisms underlying egress of apicomplexan parasites. The egress inhibitory compound, MMV676881, was originally identified by the Nluc screen as a putative invasion inhibitor since the Nluc enzyme was released from the schizonts, suggesting that schizont rupture had occurred. Giemsa stained smears, however, revealed the compound trapped merozoites inside unruptured iRBCs. We observed that the broad-spectrum cysteine protease inhibitor, E64, acts similarly to MMV676881 in the Nluc invasion assay by not preventing Nluc release. A probable explanation for the misclassification of MMV676881 is that the RBC membrane had become leaky to the Nluc reporter protein in mature schizonts, allowing it to escape into the growth medium. This agrees with findings that demonstrate RBCs are permeable to small molecules, including Nluc

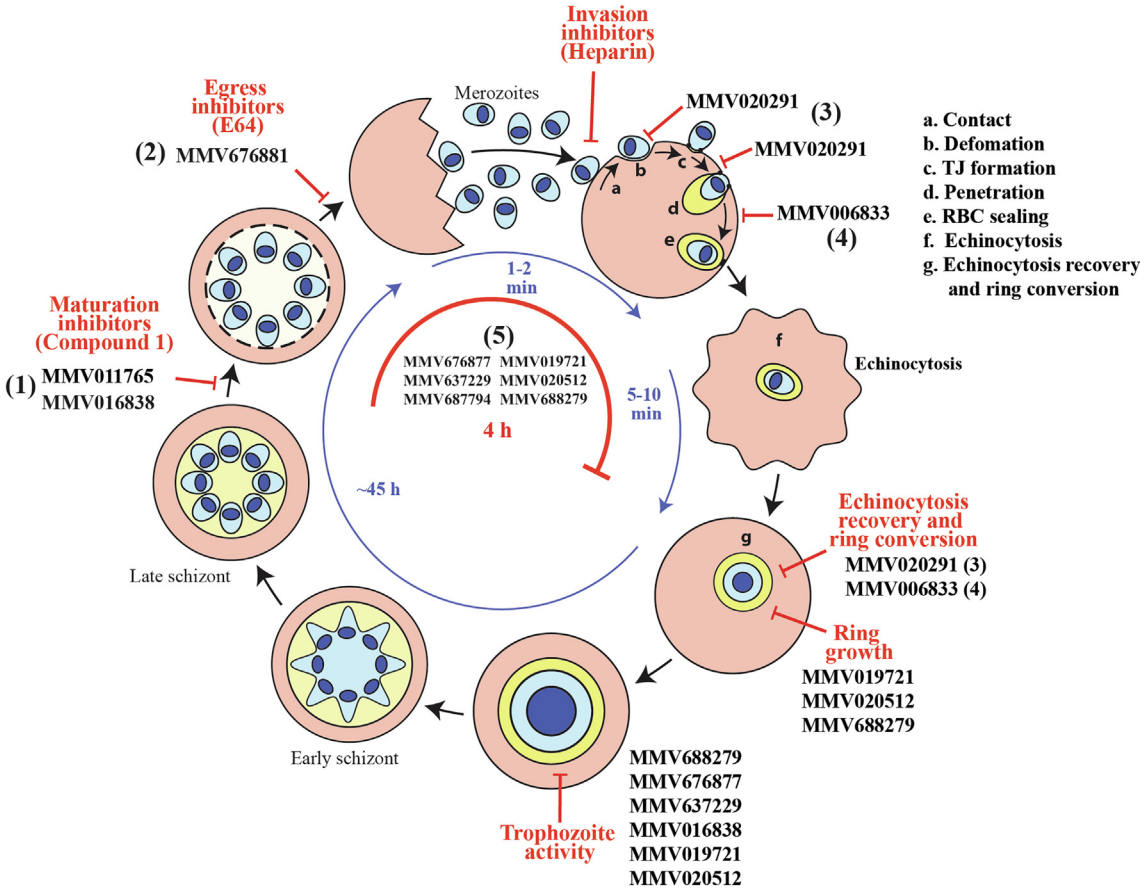


**Fig. 7.** Summary of key effects of hit compounds that inhibit egress and invasion. Schematic of proposed locations where Medicines for Malaria Venture (MMV) Pathogen Box compounds act to inhibit egress and invasion. MMV011765 and MMV016838 act to inhibit *Plasmodium falciparum* schizont maturation, resembling treatment with the cGMP dependent protein kinase G (PKG) inhibitor, Compound 1 (C1) (1). MMV676881 induces the formation of red blood cell (RBC) membrane-trapped merozoites, acting similarly to the protease inhibitor, E64 (2). MMV020291 blocks merozoite invasion by inhibiting penetration and prevents RBC recovery from echinocytosis (3). MMV006833 slows down the invasion process, prevents RBC echinocytosis recovery and blocks ring formation (4). MMV676877, MMV019721, MMV637229, MMV020512, MMV687794 and MMV688279 do not specifically block merozoite invasion or egress but may induce growth defects that indirectly hinder the invasion process (5).

reporter proteins, at late schizont stages in the presence of E64 (Glushakova et al., 2010; Collins et al., 2013; Hale et al., 2017; Absalon et al., 2018).

MMV676881 likely targets cysteine proteases as it was originally identified as an inhibitor of cruzain, a papain-like cysteine protease present in *Trypanosoma cruzi* (Mott et al., 2010; Veale, 2019). Cysteine proteases have been shown to be crucial for merozoite egress in *P. falciparum* through the use of E64 (Glushakova et al., 2009), as well as genetic manipulations of cysteine proteases such as serine rich antigen 6 (SERA6) whereby a conditional knockdown revealed it was essential for RBC membrane rupture of schizonts by reducing cytoskeletal stability (Glushakova et al., 2009; Thomas et al., 2018). Live cell microscopy and functional assays performed in this study indicated MMV676881 potentially acted as a *P. falciparum* cysteine protease inhibitor since the RBCM trapped merozoites it produced could be mechanically broken to release invasion competent merozoites.

MMV020291 and MMV006833 were the most invasion-specific inhibitors we identified in the screen. When schizonts were treated with MMV006833, MMV020291 or DMSO, no differences were observed in the number of merozoites which contacted RBCs per egress and their duration of deformation. This indicated that low affinity early interactions mediated by MSP1 and its associated proteins are likely to be unaffected by either compound (Boyle et al., 2017). RBC deformation was, however, weaker with MMV020291 treatment and did not progress to strong deformation, defined by a merozoite pushing a furrow into the RBC surface. This indicates there may be a lack of the more intense and complex levels of deformation mediated by EBA and PfRhs interactions (Tham et al., 2015; Koch et al., 2017). These observations are consistent with MMV020291 inhibiting the discharge of micronemes and/or rhoptries (Singh et al., 2010; Cowman et al., 2012).

In addition to the lack of extreme deformation, merozoites treated with MMV020291 did not appreciably migrate across the surface of the RBC, a behaviour known as gliding motility that has been observed in normal merozoite-RBC interactions (Weiss et al., 2015; Perrin et al., 2018). The actin-myosin motor is critical for deformation, motility and RBC penetration whereby merozoites treated with actin polymerisation inhibitor, cytochalasin D, have prevented migration over RBCs and failure of invasion (Miller et al., 1979; Weiss et al., 2015). MMV020291 could therefore be inhibiting the actin-myosin motor, although some functionality must be retained since many merozoites were seen to push into the RBC at the point at which echinocytosis began within the timeframe of normal invasion and were also observed to partially form a PV.

Although MMV020291 appears to inhibit strong RBC deformation, a function mediated by EBAs and PfRhs, it does not appear to inhibit the downstream-acting PfRh5. This protein is the only non-redundant PfRh and binds to the RBC receptor, basigin, that probably activates secretion of the RON complex to enable AMA1-RON2 tight junction formation (Crosnier et al., 2011; Chen et al., 2014; Weiss et al., 2015). Antibodies to PfRh5, or basigin, inhibit merozoite invasion but pre-invasion, deformation and reorientation processes remain unaffected (Weiss et al., 2015, 2016). This is not what we observed following MMV020291 treatment suggesting PfRh5 functions are not the target. PfRh5 inhibition also prevents echinocytosis from occurring, suggesting MMV020291 also functions downstream of this protein since echinocytosis clearly occurs following MMV020291 treatment. In this respect, MMV020291 more closely mimics the effects of blocking the AMA1 and RON complex interaction, where merozoites remain attached after echinocytosis was initiated and RBC recovery to its normal biconcave shape was greatly delayed (Yap et al., 2014; Weiss et al., 2016). MMV020291 therefore inhibits a range of early and late acting invasion functions making it unclear what the possible target may be.

We observed MMV020291 treated merozoites had formed protrusions at the site of contact with the RBC surface. These protrusions were stained with the same fluorescent dye that was used to label the merozoites, indicating that they originated from parasite material. These protrusions may therefore be merozoites that have differentiated into ring-stage parasites on the outside of the RBC as newly invaded merozoites often produce mobile, pseudopodial extensions within the iRBC prior to ring differentiation which can be observed in a normal invasion event in Supplementary Video S3. Live cell microscopy of failed invasion events have not been previously described to form protrusions as recently observed with PKA and adenylate cyclase beta gene disruptions (Patel et al., 2019). Further support that MMV020291 treatment causes unsuccessful merozoites to differentiate into rings is that there was no significant difference observed between the time taken for pseudopod formation to become visible on the surface of MMV020291 treated RBCs compared with normally invaded RBCs. The small, partially formed PV-like structure that was visible in some of the failed invasion sites of MMV020291 treated merozoites indicates parasite-induced modification of the RBC surface had occurred. These PV-like structures could be the equivalent of the whorl-like membranous structures that have been seen to form at the RBC surface from rhoptry contents when merozoite invasion was arrested with cytochalasin D (Riglar et al., 2011).

In contrast to MMV020291, MMV006833 treatment did not affect the ability of the merozoite to deform RBCs, form tight junctions and invade RBCs, indicating that the release of the rhoptries, micronemes and associated interactions with RBC receptors were unaffected. Whilst MMV006833 treated merozoites were able to fully enter their RBCs, the invasion process was significantly slower than normal invasion events, suggesting that the actin-myosin motor may be affected. However, treatment with MMV006833 did not affect the ability of the merozoite ability to cause severe deformation, which indicates that the actin-myosin motor can still function, as treatment with cytochalasin D has previously been shown to block deformation (Weiss et al., 2015). Once invaded, the merozoites treated with MMV006833 were observed to arrest in at the pseudopod stage, unable to differentiate into ring-stage parasites, and this may be the mechanism by which this compound blocks growth. There is little known about the mechanisms underlying merozoite differentiation into ring stage parasites post invasion and identifying the target of MMV006833 may further the study of this process.

The remaining six compounds (MMV676877, MMV637229, MMV688279, MMV687794, MMV019721 and MMV020512) from the lead list we have termed “general growth inhibitors” as whilst they inhibited schizont progression to ring-stage parasites in the primary Nluc screen, did not specifically block parasite invasion. This was corroborated by growth assays that determined five out of six of these compounds have inhibitory activity across other stages of the lifecycle (MMV676877, MMV637229, MMV688279, MMV019721 and MMV020512). Supporting this, a screen of the MMV Pathogen Box to identify stages of compound activity in the *P. falciparum* RBC 48 h lifecycle by using DNA content as a marker of stage arrest, classified these five compounds as either arresting parasite growth without DNA replication (i.e. ring stage) or halting growth at trophozoite stage without sufficient DNA replication (Tougan et al., 2019). It is therefore likely that some of these compounds could disrupt general cellular pathways such as DNA regulation or transcription and translation machinery. It has been demonstrated in schizonts that 10% of the parasite genome has a high level of transcription, with genes encoding for proteins such as MSPs, and rhoptries being upregulated in late schizogony

(Bozdech et al., 2003; Lu et al., 2017). Four hit compounds from the primary Nluc screen targeting elongation factor 2 (EF2) and DNA binding agents were removed for possessing ring stage activity and lacking novel targets in the compound triaging process (Rodríguez et al., 2008; Baragaña et al., 2015; Duffy et al., 2017). This demonstrates that agents that block DNA regulation may inadvertently inhibit essential invasion genes from being transcribed, thereby inducing invasion inhibitory phenotypes. Whilst an in silico analysis of potential molecular docking candidates to PfCDPK5 identified MMV020512 as a hit compound (Rout and Mahapatra, 2019), we have failed to observe any inhibitory phenotypes that have previously been seen with PfCDPK5 knockdowns, namely the development of RBCM trapped merozoites (Dvorin et al., 2010; Absalon et al., 2018).

The sixth of these general growth inhibitors, MMV687794, was identified as an inhibitor that arrested late trophozoite/schizont after DNA replication occurred in the aforementioned study (Tougan et al., 2019) and whilst it did not directly inhibit invasion in the purified merozoite assays, we saw no growth defects at other stages. This could indicate that this compound may block targets upstream of invasion that are required to "prime" the merozoite for invasion in the schizont stage, such as proteins that undergo proteolytic processing in schizonts such as AMA1, MSP1 and the rhoptry associated protein, RAP1 (Howard et al., 1998; Baldi et al., 2000; Silmon de Monerri et al., 2011; Das et al., 2015; Nasamu et al., 2017; Pino et al., 2017).

In conclusion, we have identified three specific merozoite egress, one RBC invasion inhibitor and one inhibitor that slows invasion and arrests ring development, in addition to several other general growth inhibitors that strongly act during the invasion stages. These inhibitors, together with their novel mechanisms of action, could complement current antimalarials which generally act on intracellular parasites during their growth phase. It will be important to identify the target proteins of the egress and invasion inhibitor compounds because this will inform structure–activity relationship based drug design to improve the potencies of compounds. Once their targets are known, these compounds could also act as useful tools to further dissect molecular details of egress and invasion processes in the parasite.

## Acknowledgements

This work was supported by the Victorian Operational Infrastructure Support Program, Australia received by the Burnet Institute, Australia. We acknowledge Medicines for Malaria Venture (MMV) for providing access to the MMV Pathogen Box and the Australian Red Cross Blood Bank for the provision of human blood. M.G.D is a recipient of an Australian Government Research Training Program Scholarship, G.E.W a Peter Doherty – Australian Biomedical Fellowship, B.E.S a Development Grant 1113712, (National Health and Medical Research Council (NHMRC)), Australia, D.W.W and B.E.S (NHMRC), Australia, Project Grant APP1143974, and T.F.dK.-W. a NHMRC Senior Research Fellowship (APP1136300). B.E.S. is a Corin Centenary Fellow (Walter and Eliza Hall Institute (WEHI)), Australia, D.W.W is a University of Adelaide, Australia, Beacon Fellow, B.S.C a Program Grant 1092789 (NHMRC). We thank Alan Cowman, WEHI, Australia, for providing the R1 peptide and Monash Micro Imaging, Australia for assistance with microscopy.

## Appendix A. Supplementary data

Supplementary data to this article can be found online at https://doi.org/10.1016/j.ijpara.2020.01.002.

## References

Absalon, S., Blomqvist, K., Rudlaff, R.M., DeLano, T.J., Pollastri, M.P., Dvorin, J.D., 2018. Calcium-dependent protein kinase 5 is required for release of egress-specific organelles in *Plasmodium falciparum*. MBio 9, e00130–00118.

Ashley, E.A., Phyo, A.P., 2018. Drugs in development for malaria. Drugs 78, 861–879.

Azevedo, M.F., Nie, C.Q., Elsworth, B., Charnaud, S.C., Sanders, P.R., Crabb, B.S., Gilson, P.R., 2014. *Plasmodium falciparum* transfected with ultra bright NanoLuc luciferase offers high sensitivity detection for the screening of growth and cellular trafficking inhibitors. PLoS ONE 9, e112571.

Baldi, D.L., Andrews, K.T., Waller, R.F., Roos, D.S., Howard, R.F., Crabb, B.S., Cowman, A.F., 2000. RAP1 controls rhoptry targeting of RAP2 in the malaria parasite *Plasmodium falciparum*. EMBO J. 19, 2435–2443.

Bannister, L.H., Hopkins, J.M., Fowler, R.E., Krishna, S., Mitchell, G.H., 2000. A brief illustrated guide to the ultrastructure of *Plasmodium falciparum* asexual blood stages. Trends Parasitol. 16, 427–433.

Bansal, A., Singh, S., More, K.R., Hans, D., Nangalia, K., Yogavel, M., Sharma, A., Chitnis, C.E., 2013. Characterization of *Plasmodium falciparum* calcium-dependent protein kinase 1 (PfCDPK1) and its role in microneme secretion during erythrocyte invasion. J. Biol. Chem. 288, 1590–1602.

Baragaña, B., Hallyburton, I., Lee, M.C.S., Norcross, N.R., Grimaldi, R., Otto, T.D., Proto, W.R., Blagborough, A.M., Meister, S., Wirjanata, G., Ruecker, A., Upton, L.M., Abraham, T.S., Almeida, M.J., Pradhan, A., Porzelle, A., Luksch, T., Martínez, M.S., Luksch, T., Bolscher, J.M., Woodland, A., Norval, S., Zuccotto, F., Thomas, J., Simeons, F., Stojanovski, L., Osuna-Cabello, M., Brock, P.M., Churcher, T.S., Sala, K.A., Zakutansky, S.E., Jiménez-Díaz, M.B., Sanz, L.M., Riley, J., Basak, R., Campbell, M., Avery, V.M., Sauerwein, R.W., Dechering, K.J., Noviyanti, R., Campo, B., Frearson, J.A., Angulo-Barturen, I., Ferrer-Bazaga, S., Gamo, F.J., Wyatt, P.G., Leroy, D., Siegl, P., Delves, M.J., Kyle, D.E., Wittlin, S., Marfurt, J., Price, R.N., Sinden, R.E., Winzeler, E.A., Charman, S.A., Bebrevska, L., Gray, D.W., Campbell, S., Fairlamb, A.H., Willis, P.A., Rayner, J.C., Fidock, D.A., Read, K.D., Gilbert, I.H., 2015. A novel multiple-stage antimalarial agent that inhibits protein synthesis. Nature 522, 315–320.

Baragaña, B., Norcross, N.R., Wilson, C., Porzelle, A., Hallyburton, I., Grimaldi, R., Osuna-Cabello, M., Norval, S., Riley, J., Stojanovski, L., Simeons, F.R.C., Wyatt, P. G., Delves, M.J., Meister, S., Duffy, S., Avery, V.M., Winzeler, E.A., Sinden, R.E., Wittlin, S., Frearson, J.A., Gray, D.W., Fairlamb, A.H., Waterson, D., Campbell, S.F., Willis, P., Read, K.D., Gilbert, I.H., 2016. Discovery of a quinoline-4-carboxamide derivative with a novel mechanism of action, multistage antimalarial activity, and potent in vivo efficacy. J. Med. Chem. 59, 9672–9685.

Blackman, M.J., Fujioka, H., Stafford, W.H.L., Sajid, M., Clough, B., Fleck, S.L., Aikawa, M., Grainger, M., Hackett, F., 1998. A Subtilisin-like protein in secretory organelles of *Plasmodium falciparum* merozoites. J. Biol. Chem. 273, 23398–23409.

Boyle, M.J., Richards, J.S., Gilson, P.R., Chai, W., Beeson, J.G., 2010a. Interactions with heparin-like molecules during erythrocyte invasion by *Plasmodium falciparum* merozoites. Blood 115 (22), 4559–4568.

Boyle, M.J., Skidmore, M., Dickerman, B., Cooper, L., Devlin, A., Yates, E., Horrocks, P., Freeman, C., Chai, W., Beeson, J.G., 2017. Identification of heparin modifications and polysaccharide inhibitors of *Plasmodium falciparum* merozoite invasion that have potential for novel drug development. Antimicrob. Agents Chemother. 61, e00709–00717.

Boyle, M.J., Wilson, D.W., Richards, J.S., Riglar, D.T., Tetteh, K.K.A., Conway, D.J., Ralph, S.A., Baum, J., Beeson, J.G., 2010b. Isolation of viable *Plasmodium falciparum* merozoites to define erythrocyte invasion events and advance vaccine and drug development. Proc. Natl. Acad. Sci. U.S.A. 107, 14378.

Bozdech, Z., Llinás, M., Pulliam, B.L., Wong, E.D., Zhu, J., DeRisi, J.L., 2003. The transcriptome of the intraerythrocytic developmental cycle of *Plasmodium falciparum*. PLoS Biol. 1, e5.

Burns, A.L., Dans, M.G., Balbin, J.M., deKoning-Ward, T.F., Gilson, P.R., Beeson, J.G., Boyle, M.J., Wilson, D.W., 2019. Targeting malaria parasite invasion of red blood cells as an antimalarial strategy. FEMS Microbiol. Rev. 43, 223.

Camus, D., Hadley, T.J., 1985. A *Plasmodium falciparum* antigen that binds to host erythrocytes and merozoites. Science 230 (4725), 553–556.

Cao, J., Kaneko, O., Thongkukiatkul, A., Tachibana, M., Otsuki, H., Gao, Q., Tsuboi, T., Torii, M., 2009. Rhoptry neck protein RON2 forms a complex with microneme protein AMA1 in *Plasmodium falciparum* merozoites. Parasitol. Int. 58, 29–35.

Chandramohanadas, R., Park, Y., Lui, L., Li, A., Quinn, D., Liew, K., Diez-Silva, M., Sung, Y., Dao, M., Lim, C.T., Preiser, P.R., Suresh, S., 2011. Biophysics of malarial parasite exit from infected erythrocytes. PLoS ONE 6, e20869.

Chen, L., Xu, Y., Healer, J., Thompson, J.K., Smith, B.J., Lawrence, M.C., Cowman, A.F., 2014. Crystal structure of PfRh5, an essential *P. falciparum* ligand for invasion of human erythrocytes. ELife 3, e04187.

Collins, C.R., Hackett, F., Atid, J., Tan, M.S.Y., Blackman, M.J., 2017. The *Plasmodium falciparum* pseudoprotease SERA5 regulates the kinetics and efficiency of malaria parasite egress from host erythrocytes. PLoS Pathog. 13 (7), e1006453.

Collins, C.R., Hackett, F., Strath, M., Penzo, M., Withers-Martinez, C., Baker, D.A., Blackman, M.J., 2013. Malaria parasite cGMP-dependent protein kinase regulates blood stage merozoite secretory organelle discharge and egress. PLoS Pathog. 9, e1003344.

Cowman, A.F., Berry, D., Baum, J., 2012. The cellular and molecular basis for malaria parasite invasion of the human red blood cell. J. Cell Biol. 198, 961–971.

Crick, A.J., Tiffert, T., Shah, S.M., Kotar, J., Lew, V.L., Cicuta, P., 2013. An automated live imaging platform for studying merozoite egress-invasion in malaria cultures. Biophys. J. 104, 997–1005.
Crosnier, C., Bustamante, L.Y., Bartholdson, S.J., Bei, A.K., Theron, M., Uchikawa, M., Mboup, S., Ndir, O., Kwiatkowski, D.P., Duraisingh, M.T., Rayner, J.C., Wright, G.J., 2011. Basigin is a receptor essential for erythrocyte invasion by *Plasmodium falciparum*. Nature 480, 534–537.
Crowther, G.J., Hillesland, H.K., Keyloun, K.R., Reid, M.C., Lafuente-Monasterio, M.J, Ghidelli-Disse, S., Leonard, S.E., He, P., Jones, J.C., Krahn, M.M., Mo, J.S., Dasari, K. S., Fox, A.M.W., Boesche, M., El Bakkouri, M., Rivas, K.L., Leroy, D., Hui, R., Drewes, G., Maly, D.J., Van Woorhis, W.C., Ojo, K.K., 2016. Biochemical Screening of Five Protein Kinases from *Plasmodium falciparum* against 14,000 Cell-Active Compounds. PloS One 11 (3), e0149996.
Das, S., Hertrich, N., Perrin, Abigail J., Withers-Martinez, C., Collins, Christine R., Jones, Matthew L., Watermeyer, Jean M., Fobes, Elmar T., Martin, Stephen R., Saibil, Helen R., Wright, Gavin J., Treeck, M., Epp, C., Blackman, Michael J., 2015. Processing of *Plasmodium falciparum* merozoite surface protein MSP1 activates a spectrin-binding function enabling parasite egress from RBCs. Cell Host Microbe 18, 433–444.
Dennis, A.S.M., Rosling, J.E.O., Lehane, A.M., Kirk, K., 2018. Diverse antimalarials from whole-cell phenotypic screens disrupt malaria parasite ion and volume homeostasis. Sci. Rep. 8 (8795). https://doi.org/10.1038/s41598-018-26819-1.
Dobrowolski, J.M., Sibley, L.D., 1996. *Toxoplasma* invasion of mammalian cells is powered by the actin cytoskeleton of the parasite. Cell 84, 933–939.
Dondorp, A.M., Nosten, F., Yi, P., Das, D., Phyo, A.P., Tarning, J., Lwin, K.M., Ariey, F., Hanpithakpong, W., Lee, S.J., Ringwald, P., Silamut, K., Imwong, M., Chotivanich, K., Lim, P., Herdman, T., An, S.S., Yeung, S., Singhasivanon, P., Day, N.P.J., Lindegardh, N., Socheat, D., White, N.J., 2009. Artemisinin resistance in *Plasmodium falciparum* malaria. N. Engl. J. Med. 361, 455–467.
Duffy, S., Sykes, M.L., Jones, A.J., Shelper, T.B., Simpson, M., Lang, R., Poulsen, S.-A., Sleebs, B.E., Avery, V.M., 2017. Screening the medicines for Malaria Venture Pathogen Box across multiple pathogens reclassifies starting points for open-source drug discovery. Antimicrob. Agents Chemother. 61, e00379–00317.
Dvorin, J.D., Martyn, D.C., Patel, S.D., Grimley, J.S., Collins, C.R., Hopp, C.S., Bright, A. T., Westenberger, S., Winzeler, E., Blackman, M.J., Baker, D.A., Wandless, T.J., Duraisingh, M.T., 2010. A plant-like kinase in *Plasmodium falciparum* regulates parasite egress from erythrocytes. Science 328, 910–912.
Fairhurst, R.M., Dondorp, A.M., 2016. Artemisinin-resistant *Plasmodium falciparum* malaria. Microbiol. Spectr. 4 (3). https://doi.org/10.1128/microbiolspec.EI10-0013-2016.
Farrow, R.E., Green, J., Katsimitsoulia, Z., Taylor, W.R., Holder, A.A., Molloy, J.E., 2011. The mechanism of erythrocyte invasion by the malarial parasite, *Plasmodium falciparum*. Semin. Cell Dev. Biol. 22, 953–960.
Gilson, P.R., Crabb, B.S., 2009. Morphology and kinetics of the three distinct phases of red blood cell invasion by *Plasmodium falciparum* merozoites. Int. J. Parasitol. 39, 91–96.
Glushakova, S., Humphrey, G., Leikina, E., Balaban, A., Miller, J., Zimmerberg, J., 2010. New stages in the program of malaria parasite egress imaged in normal and sickle erythrocytes. Curr. Biol. 20, 1117–1121.
Glushakova, S., Mazar, J., Hohmann-Marriott, M.F., Hama, E., Zimmerberg, J., 2009. Irreversible effect of cysteine protease inhibitors on the release of malaria parasites from infected erythrocytes. Cell. Microbiol. 11, 95–105.
Gonzalez, V., Combe, A., David, V., Malmquist, N.A., Delorme, V., Leroy, C., Blazquez, S., Ménard, R., Tardieux, I., 2009. Host cell entry by apicomplexa parasites requires actin polymerization in the host cell. Cell Host Microbe 5, 259–272.
Green, J.L., Moon, R.W., Whalley, D., Bowyer, P.W., Wallace, C., Rochani, A., Nageshan, R.K., Howell, S.A., Grainger, M., Jones, H.M., Ansell, K.H., Chapman, T.M., Taylor, D.L., Osborne, S.A., Baker, D.A., Tatu, U., Holder, A.A., 2016. Imidazopyridazine inhibitors of *Plasmodium falciparum* calcium-dependent protein kinase 1 also target cyclic GMP-dependent protein kinase and heat shock protein 90 to kill the parasite at different stages of intracellular development. Antimicrob. Agents Chemother. 60, 1464–1475.
Gurnett, A.M., Liberator, P.A., Dulski, P.M., Salowe, S.P., Donald, R.G.K., Anderson, J. W., Wiltsie, J., Diaz, C.A., Harris, G., Chang, B., Darkin-Rattray, S.J., Nare, B., Crumley, T., Blum, P.S., Misura, A.S., Tamas, T., Sardana, M.K., Yuan, J., Biftu, T., Schmatz, D.M., 2002. Purification and molecular characterization of cGMP-dependent protein kinase from apicomplexan parasites: a novel chemotherapeutic target. J. Biol. Chem. 277, 15913–15922.
Hale, V.L., Watermeyer, J.M., Hackett, F., Vizcay-Barrena, G., van Ooij, C., Thomas, J. A., Spink, M.C., Harkiolaki, M., Duke, E., Fleck, R.A., Blackman, M.J., Saibil, H.R., 2017. Parasitophorous vacuole poration precedes its rupture and rapid host erythrocyte cytoskeleton collapse in *Plasmodium falciparum* egress. Proc. Natl. Acad. Sci. U.S.A. 114 (13), 3439–3444.
Harris, K.S., Casey, J.L., Coley, A.M., Masciantonio, R., Sabo, J.K., Keizer, D.W., Lee, E.F., McMahon, A., Norton, R.S., Anders, R.F., Foley, M., 2005. Binding hot spot for invasion inhibitory molecules on *Plasmodium falciparum* apical membrane antigen 1. Infect. Immun. 73, 6981–6989.
Hasenkamp, S., Russell, K.T., Horrocks, P., 2012. Comparison of the absolute and relative efficiencies of electroporation-based transfection protocols for *Plasmodium falciparum*. Malar. J. 11 (210). https://doi.org/10.1186/1475-2875-11-210.
Hennessey, K.M., Rogiers, I.C., Shih, H.-W., Hulverson, M.A., Choi, R., McCloskey, M. C., Whitman, G.R., Barrett, L.K., Merritt, E.A., Paredez, A.R., Ojo, K.K., 2018. Screening of the Pathogen Box for inhibitors with dual efficacy against *Giardia lamblia* and *Cryptosporidium parvum*. PLoS Negl. Trop. Dis. 12 (8). e0006673.
Holder, A.A., Freeman, R.R., 1984. The three major antigens on the surface of *Plasmodium falciparum* merozoites are derived from a single high molecular weight precursor. J. Exp. Med. 160, 624.
Hopp, C.S., Bowyer, P.W., Baker, D.A., 2012. The role of cGMP signalling in regulating life cycle progression of *Plasmodium*. Microbes Infect. 14, 831–837.
Howard, R.F., Narum, D.L., Blackman, M., Thurman, J., 1998. Analysis of the processing of *Plasmodium falciparum* rhoptry-associated protein 1 and localization of Pr86 to schizont rhoptries and p67 to free merozoites. Mol. Biochem. Parasitol. 92, 111–122.
Iyer, G.R., Singh, S., Kaur, I., Agarwal, S., Siddiqui, M.A., Bansal, A., Kumar, G., Saini, E., Paul, G., Mohmmed, A., Chitnis, C.E., Malhotra, P., 2018. Calcium-dependent phosphorylation of *Plasmodium falciparum* serine repeat antigen 5 triggers merozoite egress. J. Biol. Chem. 293, 9736–9746.
Koch, M., Wright, K.E., Otto, O., Herbig, M., Salinas, N.D., Tolia, N.H., Satchwell, T.J., Guck, J., Brooks, N.J., Baum, J., 2017. *Plasmodium falciparum* erythrocyte-binding antigen 175 triggers a biophysical change in the red blood cell that facilitates invasion. Proc. Natl. Acad. Sci. U.S.A. 114, 4225.
Koussis, K., Withers-Martinez, C., Yeoh, S., Child, M., Hackett, F., Knuepfer, E., Juliano, L., Woehlbier, U., Bujard, H., Blackman, M.J., 2009. A multifunctional serine protease primes the malaria parasite for red blood cell invasion. EMBO J. 28, 725–735.
Lamarque, M., Besteiro, S., Papoin, J., Roques, M., Vulliez-Le Normand, B., Morlon-Guyot, J., Dubremetz, J.-F., Fauquenoy, S., Tomavo, S., Faber, B.W., Kocken, C.H., Thomas, A.W., Boulanger, M.J., Bentley, G.A., Lebrun, M., 2011. The RON2-AMA1 interaction is a critical step in moving junction-dependent invasion by apicomplexan parasites. PLoS Pathog. 7, e1001276.
Lanzillotti, R., Coetzer, T.L., 2006. The 10 kDa domain of human erythrocyte protein 4.1 binds the *Plasmodium falciparum* EBA-181 protein. Malar. J. 5 (100). https://doi.org/10.1186/1475-2875-5-100.
Le Manach, C., Nchinda, A.T., Paquet, T., Gonzàlez Cabrera, D., Younis, Y., Han, Z., Bashyam, S., Zabiulla, M., Taylor, D., Lawrence, N., White, K.L., Charman, S.A., Waterson, D., Witty, M.J., Wittlin, S., Botha, M.E., Nondaba, S.H., Reader, J., Birkholtz, L.-M., Jiménez-Díaz, M.B., Martínez, M.S., Ferrer, S., Angulo-Barturen, I., Meister, S., Antonova-Koch, Y., Winzeler, E.A., Street, L.J., Chibale, K., 2016. Identification of a potential antimalarial drug candidate from a series of 2-aminopyrazines by optimization of aqueous solubility and potency across the parasite life cycle. J. Med. Chem. 59, 9890–9905.
Li, X., Marinkovic, M., Russo, C., McKnight, C.J., Coetzer, T.L., Chishti, A.H., 2012. Identification of a specific region of *Plasmodium falciparum* EBL-1 that binds to host receptor glycophorin B and inhibits merozoite invasion in human red blood cells. Mol. Biochem. Parasitol. 183, 23–31.
Lin, C.S., Uboldi, A.D., Marapana, D., Czabotar, P.E., Epp, C., Bujard, H., Taylor, N.L., Perugini, M.A., Hodder, A.N., Cowman, A.F., 2014. The merozoite surface protein 1 complex is a platform for binding to human erythrocytes by *Plasmodium falciparum*. J. Biol. Chem. 289, 25655–25669.
Lu, X.M., Batugedara, G., Lee, M., Prudhomme, J., Bunnik, E.M., Le Roch, K.G., 2017. Nascent RNA sequencing reveals mechanisms of gene regulation in the human malaria parasite *Plasmodium falciparum*. Nucleic Acids Res. 45, 7825–7840.
Mayer, D.C.G., Kaneko, O., Hudson-Taylor, D.E., Reid, M.E., Miller, L.H., 2001. Characterization of a *Plasmodium falciparum* erythrocyte-binding protein paralogous to EBA-175. Proc. Natl. Acad. Sci. U.S.A. 98, 5222–5227.
Miller, L.H., Masmichi, A., Johnson, J.G., Shiroishi, T., 1979. Interaction between cytochalasin B-treated malarial parasites and erythrocytes. Attachment and junction formation. J. Exp. Med. 149, 172–184.
Mott, B.T., Ferreira, R.S., Simeonov, A., Jadhav, A., Ang, K.K.-H., Leister, W., Shen, M., Silveira, J.T., Doyle, P.S., Arkin, M.R., McKerrow, J.H., Inglese, J., Austin, C.P., Thomas, C.J., Shoichet, B.K., Maloney, D.J., 2010. Identification and optimization of inhibitors of Trypanosomal cysteine proteases: cruzain, rhodesain, and TbCatB. J. Med. Chem. 53, 52–60.
Nasamu, A.S., Glushakova, S., Russo, I., Vaupel, B., Oksman, A., Kim, A.S., Fremont, D. H., Tolia, N., Beck, J.R., Meyers, M.J., Niles, J.C., Zimmerberg, J., Goldberg, D.E., 2017. Plasmepsins IX and X are essential and druggable mediators of malaria parasite egress and invasion. Science 358, 518.
Nugraha, A.B., Tuvshintulga, B., Guswanto, A., Tayebwa, D.S., Rizk, M.A., Gantuya, S., El-Saber Batiha, G., Beshbishy, A.M., Sivakumar, T., Yokoyama, N., Igarashi, I., 2019. Screening the medicines for Malaria Venture Pathogen Box against piroplasm parasites. Int. J. Parasitol. Drugs Drug Resist. 10, 84–90.
Nyagwange, J., Awino, E., Tijhaar, E., Svitek, N., Pelle, R., Nene, V., 2019. Leveraging the Medicines for Malaria Venture malaria and pathogen boxes to discover chemical inhibitors of East Coast fever. Int. J. Parasitol. Drugs Drug Resist. 9, 80–86.
Paquet, T., Le Manach, C., Cabrera, D.G., Younis, Y., Henrich, P.P., Abraham, T.S., Lee, M.C.S., Basak, R., Ghidelli-Disse, S., Lafuente-Monasterio, M.J., Bantscheff, M., Ruecker, A., Blagborough, A.M., Zakutansky, S.E., Zeeman, A.-M., White, K.L., Shackleford, D.M., Mannila, J., Morizzi, J., Scheurer, C., Angulo-Barturen, I., Martínez, M.S., Ferrer, S., Sanz, L.M., Gamo, F.J., Reader, J., Botha, M., Dechering, K.J., Sauerwein, R.W., Tungtaeng, A., Vanachayangkul, P., Lim, C.S., Burrows, J., Witty, M.J., Marsh, K.C., Bodenreider, C., Rochford, R., Solapure, S.M., Jiménez-Díaz, M.B., Wittlin, S., Charman, S.A., Donini, C., Campo, B., Birkholtz, L.-M., Hanson, K.K., Drewes, G., Kocken, C.H.M., Delves, M.J., Leroy, D., Fidock, D.A., Waterson, D., Street, L.J., Chibale, K., 2017. Antimalarial efficacy of MMV390048, an inhibitor of *Plasmodium* phosphatidylinositol 4-kinase. Sci. Transl. Med. 9 (387), eaad9735.
Patel, A., Perrin, A.J., Flynn, H.R., Bisson, C., Withers-Martinez, C., Treeck, M., Flueck, C., Nicastro, G., Martin, S.R., Ramos, A., Gilberger, T.W., Snijders, A.P., Blackman,

M.J., Baker, D.A., 1999. Cyclic AMP signalling controls key components of malaria parasite host cell invasion machinery. PLoS Biol. 17, e3000264.
Perrin, A.J., Collins, C.R., Russell, M.R.G., Collinson, L.M., Baker, D.A., Blackman, M.J., 2018. The actinomyosin motor drives malaria parasite red blood cell invasion but not egress. MBio 9, e00905–00918.
Pino, P., Caldelari, R., Mukherjee, B., Vahokoski, J., Klages, N., Maco, B., Collins, C.R., Blackman, M.J., Kursula, I., Heussler, V., Brochet, M., Soldati-Favre, D., 2017. A multi-stage antimalarial targets the plasmepsins IX and X essential for invasion and egress. Science 358, 522–528.
Richard, D., MacRaild, C.A., Riglar, D.T., Chan, J.-A., Foley, M., Baum, J., Ralph, S.A., Norton, R.S., Cowman, A.F., 2010. Interaction between *Plasmodium falciparum* apical membrane antigen 1 and the rhoptry neck protein complex defines a key step in the erythrocyte invasion process of malaria parasites. J. Biol. Chem. 285, 14815–14822.
Riglar, D.T., Richard, D., Wilson, D.W., Boyle, M.J., Dekiwadia, C., Turnbull, L., Angrisano, F., Marapana, D.S., Rogers, K.L., Whitchurch, C.B., Beeson, J.G., Cowman, A.F., Ralph, S.A., Baum, J., 2011. Super-resolution dissection of coordinated events during malaria parasite invasion of the human erythrocyte. Cell Host Microbe 9, 9–20.
Rodríguez, F., Rozas, I., Kaiser, M., Brun, R., Nguyen, B., Wilson, W.D., García, R.N., Dardonville, C., 2008. New bis(2-aminoimidazoline) and bisguanidine DNA minor groove binders with potent in vivo antitrypanosomal and antiplasmodial activity. J. Med. Chem. 51, 909–923.
Rout, S., Mahapatra, R.K., 2019. In silico analysis of *Plasmodium falciparum* CDPK5 protein through molecular modeling, docking and dynamics. J. Theor. Biol. 461, 254–267.
Ruecker, A., Shea, M., Hackett, F., Suarez, C., Hirst, E.M.A., Milutinovic, K., Withers-Martinez, C., Blackman, M.J., 2012. Proteolytic activation of the essential parasitophorous vacuole cysteine protease SERA6 accompanies malaria parasite egress from its host erythrocyte. J. Biol. Chem. 287, 37949–37963.
Sajid, M., Withers-Martinez, C., Blackman, M.J., 2000. Maturation and specificity of *Plasmodium falciparum* subtilisin-like protease-1, a malaria Merozoite Subtilisin-like serine protease. J. Biol. Chem. 275, 631–641.
Sam-Yellowe, T.Y., 1996. Rhoptry organelles of the apicomplexa: their role in host cell invasion and intracellular survival. Parasitol. Today 12, 308–316.
Silmon de Monerri, N.C., Flynn, H.R., Campos, M.G., Hackett, F., Koussis, K., Withers-Martinez, C., Skehel, J.M., Blackman, M.J., 2011. Global identification of multiple substrates for *Plasmodium falciparum* SUB1, an essential malarial processing protease. Infect. Immun. 79, 1086–1097.
Singh, S., Alam, M.M., Pal-Bhowmick, I., Brzostowski, J.A., Chitnis, C.E., 2010. Distinct external signals trigger sequential release of apical organelles during erythrocyte invasion by malaria parasites. PLoS Pathog. 6 (2), e1000746.
Spalenka, J., Escotte-Binet, S., Bakiri, A., Hubert, J., Renault, J.-H., Velard, F., Duchateau, S., Aubert, D., Huguenin, A., Villena, I., 2018. Discovery of new inhibitors of *Toxoplasma gondii* via the pathogen box. Antimicrob. Agents Chemother. 62, e01640–01617.
Spillman, N.J., Kirk, K., 2015. The malaria parasite cation ATPase PfATP4 and its role in the mechanism of action of a new arsenal of antimalarial drugs. Int. J. Parasitol. Drugs Drug Resist. 5, 149–162.
Subramanian, G., Belekar, M.A., Shukla, A., Tong, J.X., Sinha, A., Chu, T.T.T., Kulkarni, A.S., Preiser, P.R., Reddy, D.S., Tan, K.S.W., Shanmugam, D., Chandramohanadas, R., 2018. Targeted phenotypic screening in *Plasmodium falciparum* and *Toxoplasma gondii* reveals novel modes of action of medicines for malaria venture malaria box molecules. mSphere 3, e00534–00517.
Taylor, H.M., McRobert, L., Grainger, M., Sicard, A., Dluzewski, A.R., Hopp, C.S., Holder, A.A., Baker, D.A., 2010. The malaria parasite cyclic GMP-dependent protein kinase plays a central role in blood-stage schizogony. Eukaryotic Cell 9, 37–45.
Tham, W.-H., Lim, N.T.Y., Weiss, G.E., Lopaticki, S., Ansell, B.R.E., Bird, M., Lucet, I., Dorin-Semblat, D., Doerig, C., Gilson, P.R., Crabb, B.S., Cowman, A.F., 2015. *Plasmodium falciparum* adhesins play an essential role in signalling and activation of invasion into human erythrocytes. PLoS Pathog. 11, e1005343.
Thomas, J.A., Tan, M.S.Y., Bisson, C., Borg, A., Umrekar, T.R., Hackett, F., Hale, V.L., Vizcay-Barrena, G., Fleck, R.A., Snijders, A.P., Saibil, H.R., Blackman, M.J., 2018. A protease cascade regulates release of the human malaria parasite *Plasmodium falciparum* from host red blood cells. Nat. Microbiol. 3, 447–455.
Tong, J.X., Chandramohanadas, R., Tan, K.S.-W., 2018. High-content screening of the medicines for Malaria Venture Pathogen Box for *Plasmodium falciparum* digestive vacuole-disrupting molecules reveals valuable starting points for drug discovery. Antimicrob. Agents Chemother. 62, e02031–02017.
Tougan, T., Toya, Y., Uchihashi, K., Horii, T., 2019. Application of the automated haematology analyzer XN-30 for discovery and development of anti-malarial drugs. Malar. J. 18, 8.
Trager, W., Jensen, J.B., 1976. Human malaria parasites in continuous culture. Science 193, 673–675.
Van Voorhis, W.C., Adams, J.H., Adelfio, R., Ahyong, V., Akabas, M.H., Alano, P., Alday, A., Alemán Resto, Y., Alsibaee, A., Alzualde, A., Andrews, K.T., Avery, S.V., Avery, V.M., Ayong, L., Baker, M., Baker, S., Ben Mamoun, C., Bhatia, S., Bickle, Q., Bounaadja, L., Bowling, T., Bosch, J., Boucher, L.E., Boyom, F.F., Brea, J., Brennan, M., Burton, A., Caffrey, C.R., Camarda, G., Carrasquilla, M., Carter, D., Belen Cassera, M., Chih-Chien Cheng, K., Chindaudomsate, W., Chubb, A., Colon, B.L., Colón-López, D.D., Corbett, Y., Crowther, G.J., Cowan, N., D'Alessandro, S., Le Dang, N., Delves, M., DeRisi, J.L., Du, A.Y., Duffy, S., Abd El-Salam El-Sayed, S., Ferdig, M.T., Fernández Robledo, J.A., Fidock, D.A., Florent, I., Fokou, P.V.T., Galstian, A., Gamo, F.J., Gokool, S., Gold, B., Golub, T., Goldgof, G.M., Guha, R., Guiguemde, W.A., Gural, N., Guy, R.K., Hansen, M.A.E., Hanson, K.K., Hemphill, A., Hooft van Huijsduijnen, R., Horii, T., Horrocks, P., Hughes, T.B., Huston, C., Igarashi, I., Ingram-Sieber, K., Itoe, M.A., Jadhav, A., Naranuntarat Jensen, A., Jensen, L.T., Jiang, R.H.Y., Kaiser, A., Keiser, J., Ketas, T., Kicka, S., Kim, S., Kirk, K., Kumar, V.P., Kyle, D.E., Lafuente, M.J., Landfear, S., Lee, N., Lee, S., Lehane, A.M., Li, F., Little, D., Liu, L., Llinás, M., Loza, M.I., Lubar, A., Lucantoni, L., Lucet, I., Maes, L., Mancama, D., Mansour, N.R., March, S., McGowan, S., Medina Vera, I., Meister, S., Mercer, L., Mestres, J., Mfopa, A.N., Misra, R.N., Moon, S., Moore, J.P., Morais Rodrigues da Costa, F., Müller, J., Muriana, A., Nakazawa Hewitt, S., Nare, B., Nathan, C., Narraidoo, N., Nawaratna, S., Ojo, K.K., Ortiz, D., Panic, G., Papadatos, G., Parapini, S., Patra, K., Pham, N., Prats, S., Plouffe, D.M., Poulsen, S.-A., Pradhan, A., Quevedo, C., Quinn, R.J., Rice, C.A., Abdo Rizk, M., Ruecker, A., St. Onge, R., Salgado Ferreira, R., Samra, J., Robinett, N.G., Schlecht, U., Schmitt, M., Silva Villela, F., Silvestrini, F., Sinden, R., Smith, D.A., Soldati, T., Spitzmüller, A., Stamm, S.M., Sullivan, D.J., Sullivan, W., Suresh, S., Suzuki, B.M., Suzuki, Y., Swamidass, S.J., Taramelli, D., Tchokouaha, L.R.Y., Theron, A., Thomas, D., Tonissen, K.F., Townson, S., Tripathi, A.K., Trofimov, V., Udenze, K.O., Ullah, I., Vallieres, C., Vigil, E., Vinetz, J.M., Voong Vinh, P., Vu, H., Watanabe, N.-a., Weatherby, K., White, P.M., Wilks, A.F., Winzeler, E.A., Wojcik, E., Wree, M., Wu, W., Yokoyama, N., Zollo, P.H.A., Abla, N., Blasco, B., Burrows, J., Laleu, B., Leroy, D., Spangenberg, T., Wells, T., Willis, P.A., 2016. Open source drug discovery with the malaria box compound collection for neglected diseases and beyond. PLoS Pathog. 12, e1005763.
Veale, C.G.L., 2019. Unpacking the pathogen box—an open source tool for fighting neglected tropical disease. ChemMedChem 14, 386–453.
Vijaykadga, S., Rojanawatsirivej, C., Cholpol, S., Phoungmanee, D., Nakavej, A., Wongsrichanalai, C., 2006. In vivo sensitivity monitoring of mefloquine monotherapy and artesunate–mefloquine combinations for the treatment of uncomplicated falciparum malaria in Thailand in 2003. Trop. Med. Int. Health 11, 211–219.
Vogt, Anna M., Winter, G., Wahlgren, M., Spillmann, D., 2004. Heparan sulphate identified on human erythrocytes: a *Plasmodium falciparum* receptor. Biochem. J. 381, 593–597.
Wang, X., Miyazaki, Y., Inaoka, D.K., Hartuti, E.D., Watanabe, Y.-I., Shiba, T., Harada, S., Saimoto, H., Burrows, J.N., Benito, F.J.G., Nozaki, T., Kita, K., 2019. Identification of *Plasmodium falciparum* mitochondrial malate: quinone oxidoreductase inhibitors from the pathogen box. Genes (Basel) 10, 471.
Weiss, G.E., Crabb, B.S., Gilson, P.R., 2016. Overlaying molecular and temporal aspects of malaria parasite invasion. Trends Parasitol. 32, 284–295.
Weiss, G.E., Gilson, P.R., Taechalertpaisarn, T., Tham, W.-H., de Jong, N.W.M., Harvey, K.L., Fowkes, F.J.I., Barlow, P.N., Rayner, J.C., Wright, G.J., Cowman, A.F., Crabb, B. S., 2015. Revealing the sequence and resulting cellular morphology of receptor-ligand interactions during *Plasmodium falciparum* invasion of erythrocytes. PLoS Pathog. 11, e1004670.
Wickham, M.E., Culvenor, J.G., Cowman, A.F., 2003. Selective inhibition of a two-step egress of malaria parasites from the host erythrocyte. J. Biol. Chem. 278, 37658–37663.
Wilson, D.W., Goodman, C.D., Sleebs, B.E., Weiss, G.E., de Jong, N.W., Angrisano, F., Langer, C., Baum, J., Crabb, B.S., Gilson, P.R., McFadden, G.I., Beeson, J.G., 2015. Macrolides rapidly inhibit red blood cell invasion by the human malaria parasite, *Plasmodium falciparum*. BMC Biol. 13 (52).
Wilson, D.W., Langer, C., Goodman, C.D., McFadden, G.I., Beeson, J.G., 2013. Defining the timing of action of antimalarial drugs against *Plasmodium falciparum*. Antimicrob. Agents Chemother. 57, 1455–1467.
World Health Organization, 2019. World Malaria Report 2019. WHO Press, Geneva, Switzerland.
Yap, A., Azevedo, M.F., Gilson, P.R., Weiss, G.E., O'Neill, M.T., Wilson, D.W., Crabb, B. S., Cowman, A.F., 2014. Conditional expression of apical membrane antigen 1 in *Plasmodium falciparum* shows it is required for erythrocyte invasion by merozoites. Cell. Microbiol. 16, 642–656.
Yeoh, S., O'Donnell, R.A., Koussis, K., Dluzewski, A.R., Ansell, K.H., Osborne, S.A., Hackett, F., Withers-Martinez, C., Mitchell, G.H., Bannister, L.H., Bryans, J.S., Kettleborough, C.A., Blackman, M.J., 2007. Subcellular discharge of a serine protease mediates release of invasive malaria parasites from host erythrocytes. Cell 131, 1072–1083.
Younis, Y., Douelle, F., Feng, T.-S., Cabrera, D.G., Manach, C.L., Nchinda, A.T., Duffy, S., White, K.L., Shackleford, D.M., Morizzi, J., Mannila, J., Katneni, K., Bhamidipati, R., Zabiulla, K.M., Joseph, J.T., Bashyam, S., Waterson, D., Witty, M.J., Hardick, D., Wittlin, S., Avery, V., Charman, S.A., Chibale, K., 2012. 3,5-diaryl-2-aminopyridines as a novel class of orally active antimalarials demonstrating single dose cure in mice and clinical candidate potential. J. Med. Chem. 55, 3479–3487.
Zhang, C., Ondeyka, J.G., Herath, K.B., Guan, Z., Collado, J., Pelaez, F., Leavitt, P.S., Gurnett, A., Nare, B., Liberator, P., Singh, S.B., 2006. Highly substituted terphenyls as inhibitors of parasite cGMP-dependent protein kinase activity. J. Nat. Prod. 69, 710–712.
Zhang, J.-H., Chung, T.D.Y., Oldenburg, K.R., 1999. A simple statistical parameter for use in evaluation and validation of high throughput screening assays. J. Biomol. Screen. 4, 67–73.